Development of hybrid TiO_2/SWCNT photocatalysts

Rita Ruivo Neves Marques

Dissertation presented for the Master Degree in the
Chemical Engineering Department at the Faculty of Engineering,
University of Porto, Portugal

Supervisors:

Prof. Joaquim Luís Bernardes Martins de Faria

Dr. Adrián Manuel Tavares da Silva

LCM - Laboratory of Catalysis and Materials
Associated Laboratory LSRE/LCM
Department of Chemical Engineering
Faculty of Engineering
University of Porto
Portugal

July 2009

Agradecimentos

A realização deste trabalho só foi possível com a contribuição de várias pessoas a quem gostaria de agradecer.

Em especial ao Professor Doutor Joaquim Faria pela supervisão deste trabalho, em particular pela preciosa ajuda na discussão científica e algumas vezes filosófica dos meus resultados. Também pelo espírito de equipa que fomenta dentro do grupo.

Ao meu co-orientador, o Doutor Adrián Silva, pelo empenho incondicional no meu trabalho e por todos os ensinamentos humanos que vão muito para além da investigação científica e que tanto para ela contribuem.

Ao Professor Doutor José Luís Figueiredo por ter disponibilizado todos os recursos técnicos do Laboratório de Catálise e Materiais, do qual é director.

A todos os meus colegas de laboratório, em especial ao Doutor Bruno Machado pela incansável ajuda em muito do que envolve a elaboração desta tese.

Aos meus colegas das *Faria Sessions* pelo seu contributo na discussão dos meus resultados: Cristina, João, Sónia e Wang.

Ao Doutor Rui Boaventura por ter disponibilizado o equipamento com o qual determinei o carbono orgânico total de algumas amostras. À Liliana pela sempre voluntariosa ajuda nessas análises.

Ao Doutor Goran Dražić pela realização das análises de HRTEM.

"The financial support under the Clean Water project is acknowledged. Clean Water is a Collaborative Project (Grant Agreement number 227017) co-funded by the Research DG of the European Commission within the joint RTD activities of the Environment and NMP Thematic Priorities."

Finalmente, à minha mãe e ao meu pai, Judite e Fernando, ao meu irmão João e à minha avó Lucília. Por tudo, sempre!

Abstract

Carbon nanotubes (CNT) have been widely used in catalytic applications due to their interesting and unique physical and chemical properties, such as high mechanical and thermal resistance. Synthesis of titanium dioxide with incorporation of CNT yields photocatalytic materials capable of absorbing visible light. This behaviour is of great interest since TiO_2 absorbs preferentially on the UV region, which merely represents 3-6 % of solar radiation. Hence, the use of CNT/TiO_2 composite materials in photocatalytic processes can result in a better usage of the sun, as it is a natural source of light. In the present work, Single-Walled Carbon Nanotubes (SWCNT) are chemically modified to be incorporated on TiO_2 matrix for further development of hybrid SWCNT/TiO_2 composites.

The surface chemistry of SWCNT is finely tailored by a HNO_3 hydrothermal method. Temperature Programmed Desorption analysis is used to determine the nature and amount of different oxygenated functionalities, which are introduced in a controlled mode, being correlated with HNO_3 concentration by a mathematical function. Operating temperature and HNO_3 concentration are key parameters in the modification of the SWCNT surface chemistry. The effect of the HNO_3 hydrothermal functionalization strongly depends on the texture of the carbon materials that are used.

Bare TiO_2 and different SWCNT/TiO_2 composites are synthesized by an acid-catalyzed sol-gel method and some selected materials are modified by means of a hydrothermal treatment. Diffuse reflectance UV-Vis spectroscopy and BET surface area measurements are used to characterize all the prepared materials which are further used in the photocatalytic oxidative degradation of two probe organic molecules (*p*-Methoxyphenol and *p*-Cyanophenol). The photocatalytic performance of SWCNT/TiO_2 composites seems to be affected by previous functionalization of SWCNT. The hydrothermal treatment improves visible light response in photocatalysis but the characterization methods used in the present study are not sufficient to explain the obtained results. Further studies are needed to optimize the development of hybrid SWCNT/TiO_2 catalysts. Suggestions to future work on SWCNT functionalization, materials preparation and photocatalytic tests are given.

Keywords: carbon nanotubes, surface chemistry, hydrothermal treatment, titania based composites, photocatalysis.

Resumo

Os nanotubos de carbono têm sido amplamente utilizados no domínio científico da catálise devido às características singulares que apresentam, tais como elevadas resistências mecânica e térmica. A síntese de dióxido de titânio (TiO_2) com incorporação de nanotubos na sua matriz resulta na obtenção de materiais activos em fotocatálise com absorção de luz na região do visível (Vis). Esta particularidade é de grande interesse prático uma vez que o TiO_2 absorve preferencialmente na região do ultravioleta (UV), o que representa apenas 3-6 % da radiação solar. Por este motivo, a utilização de materiais compósitos do tipo CNT/TiO_2 em processos fotocatalíticos pode resultar num melhor aproveitamento da radiação solar como fonte natural de luz. Nesta tese, nanotubos de carbono de parede única (*Single-Walled Carbon Nanotubes* – SWCNT) são modificados quimicamente e posteriormente incorporados numa matriz de TiO_2, formando materiais compósitos do tipo SWCNT/TiO_2.

A química de superfície dos SWCNT é modificada de uma forma controlada através de um tratamento hidrotérmico com ácido nítrico, sendo a natureza e quantidade dos grupos oxigenados introduzidos determinadas por desorção a temperatura programada. A quantidade de grupos introduzidos na superfície dos SWCNT é correlacionada com a concentração de ácido nítrico por uma função matemática. Neste estudo, conclui-se que os parâmetros chave para a modificação controlada da química de superfície dos SWCNT são a temperatura de operação e a concentração de ácido nítrico. Conclui-se também que a funcionalização de um material de carbono por tratamento hidrotérmico com ácido nítrico é fortemente influenciado pela sua morfologia.

A preparação de TiO_2 e de compósitos do tipo SWCNT/TiO_2 é feita com base num método sol-gel catalisado em meio ácido. Alguns destes materiais foram seleccionados e sujeitos a um tratamento hidrotérmico. Todos estes catalisadores são caracterizados por espectroscopia de reflectância difusa na região do UV-Vis e pela área específica BET, sendo posteriormente utilizados na fotodegradação oxidativa de duas moléculas orgânicas (*p*-Methoxyphenol e *p*-Cyanophenol). A funcionalização prévia dos SWCNT parece ter influência no comportamento fotocatalítico dos compósitos SWCNT/TiO_2. Verifica-se também que o tratamento hidrotérmico aumenta a resposta fotocatalítica na região do visível. No entanto, os métodos de caracterização utilizados neste estudo não são suficientes para explicar os resultados obtidos. São necessários estudos posteriores para a optimização dos catalisadores SWCNT/TiO_2. Nesse sentido, são apresentadas sugestões de trabalho futuro no âmbito da funcionalização dos SWCNT, da preparação de materiais e dos ensaios de fotocatálise.

Palavras-chave: nanotubos de carbono, química de superfície, tratamento hidrotérmico, compósitos de TiO_2, fotocatálise.

Table of Contents

List of Figures

List of Tables

Glossary

Notations

C	Pollutant concentration	mol L^{-1}
C_0	Initial pollutant concentration	mol L^{-1}
S_{BET}	Specific Surface Area	m^2/g
TOC	Total Organic Carbon	mg L^{-1}

Acronyms

CB	Electronic Conduction Band
CNT	Carbon Nanotubes
CVD	Chemical Vapor Deposition
DR UV-Vis	Diffuse Reflectance of UV-Vis
EDXS	Energy-Dispersive X-ray Spectrometer analysis
HPLC	High Performance Liquid Chromatography
HRTEM	High Resolution Transmission Electron Microscopy
HT	Hydrothermal Treatment
KM	Kubelka-Munk units
MWCNT	Multi-Walled Carbon Nanotubes
SAED	Selected Area Electron Diffraction
SG	Sol-Gel
SWCNT	Single-Walled Carbon Nanotubes
TGA	Thermogravimetric Analysis
TOC	Total Organic Carbon
TPD	Temperature Programmed Desorption
UV	Ultra Violet Radiation
VB	Electronic Valence Band
Vis	Visible Radiation
WL	Weight Loss

Aim of the work and thesis outline

Over the past 30 years, the number of people affected by droughts and water scarcity in Europe has increased about 20%. Higher standards of living are resulting in a growing consumption of water and, simultaneously, water quality concerns. The development of new clean technologies in this domain is becoming mandatory. Due to the fast advances on light related technologies, heterogeneous photocatalysis is being positioned as one of the most popular oxidation techniques in waste water treatment. Titanium dioxide (TiO_2) is the most used catalyst in photocatalysis due to its high efficiency in oxidative degradation under UV light. However, TiO_2 response in the visible range of the spectrum is limited because of its natural band-gap. This behaviour is truly a drawback when intending to use natural solar radiation in photocatalytic processes, since merely ca. 3-6 % of solar radiation consists of UV light. A possible solution is to modify TiO_2, in order to obtain composite photocatalysts with an overall narrower band gap, thus taking benefit of the sun, as it is a natural source of light for the photocatalytic process. In fact, it has been reported in literature that TiO_2 composites containing a carbon phase, in particular carbon nanotubes (CNT), can show visible response in photocatalysis. Ballistic transport properties of Single-Walled Carbon Nanotubes (SWCNT) can be especially advantageous by reducing the electron /hole (e^-/h^+) recombination rate in the photocatalytic process. In this context, the investigation undertaken for this thesis is focused on a first particular step of the development of SWCNT/TiO_2 composite photocatalysts, which is the controlled modification of the SWCNT surface chemistry. The latter is thought to be important in the further integration of SWCNT on TiO_2 matrices. Some composite materials are prepared and preliminary tests are performed on the photocatalytic oxidative degradation of two organic probe molecules (*p*-Methoxyphenol and *p*-Cyanophenol). It is worth to note that this work is at the starting point of a broader European project and the research will progress with further optimization of several parameters.

This thesis includes 5 mains sections, being the first one an introduction to the main topics: photocatalysis and composite CNT/TiO_2 photocatalysts and functionalization of SWCNT. Section 2 describes the experimental procedure, characterization methods and analytical techniques employed on functionalization of SWCNT, preparation of the SWCNT/TiO_2 composites and photocatalytic tests. The results obtained are presented and discussed on section 3. Sections 4 and 5 are respectively dedicated to the final conclusions and suggestions for future work.

1 Introduction

1.1 Photocatalysis and CNT/TiO_2 composite catalysts

Growing water quality concerns have been resulting in strictly legislation on the emission of several harmful substances to water courses. The EU Commission Services have recently proposed a directive defining new Environmental Quality Standards (EQS) for hazardous priority substances [1]. Consequently, new clean technologies have been developed in the context of waste water treatment. Heterogeneous photocatalysis is earning a growing relevance amongst several oxidation techniques, due to the last advances in light related technologies [2-4].

The photocatalytic degradation of an organic pollutant is a chemical process in which various components take part: a reactant, a photon with the appropriated energy, a catalyst surface (normally a semiconductor) and a strong oxidizing agent [5]. Some misconceptions are involved around photocatalysis like the role of light in the reaction mechanism. It is worth to emphasize that light acts as a reactant and not as a catalyst. Heterogeneous photocatalysis is a catalytic process which includes several sequential steps: diffusion of the reactants from the bulk phase to the catalyst surface, adsorption of at least one of the reactants, reaction in the adsorbed phase and desorption of the products from the catalyst surface [5]. When photons are firstly absorbed by the substrate molecule, the process is named as photocatalytic reaction or catalyzed photoreaction. On the other hand, if the irradiated light is absorbed firstly by the catalyst, the process is referred as sensitized photoreaction [6]. The interest on searching for the optimum catalyst in photocatalytic applications requires that the process occurs under a photosensitized reaction, with no caption of light by the substrate molecule. The intensity of the light irradiated must be enough to overcome the energy of the band gap of the catalyst. Since the catalyst is irradiated with higher energy than that of the band gap, the electrons become excited from the valence band (VB, Highest Occupied Molecular Orbital - HOMO) to the conduction band (CB, Lowest Unoccupied Molecular Orbital - LUMO) generating electron/hole (e^-/h^+) pairs. These agents will get involved in a sequence of redox reactions generating highly oxidizing species like hydroxyl radicals ($HO^\bullet$) and superoxide radicals ($O_2^{\bullet -}$).

Titanium dioxide (TiO_2) is the preferred catalyst to be used in photocatalysis not just because of its high efficiency producing e^-/h^+ pairs under UV light but also for other important reasons: it is a chemically stable and a low cost material. Photocatalytic active TiO_2 powders can be easily synthesized by means of the sol-gel method [7, 8]. This preparation technique

involves the use of a metal alkoxide as a precursor which is dissolved in an alcohol. The alkoxide is hydrolyzed and then the condensation of the polymeric chains takes place. The resulting gel is allowed to dry under ambient or supercritical conditions forming a xerogel or an aerogel, respectively. Further calcination helps to eliminate the remaining solvent and, at different calcination temperatures, distinct crystalline phases can be attained. Very homogeneous materials are obtained using the sol-gel synthesis procedure and the possibility to include other phases in the titania matrix is an additional advantage. There are three polymorphs of TiO_2 that can be found in nature: anatase (Fig. 1.1a), rutile (Fig. 1.1b) and brookite (Fig. 1.1c).

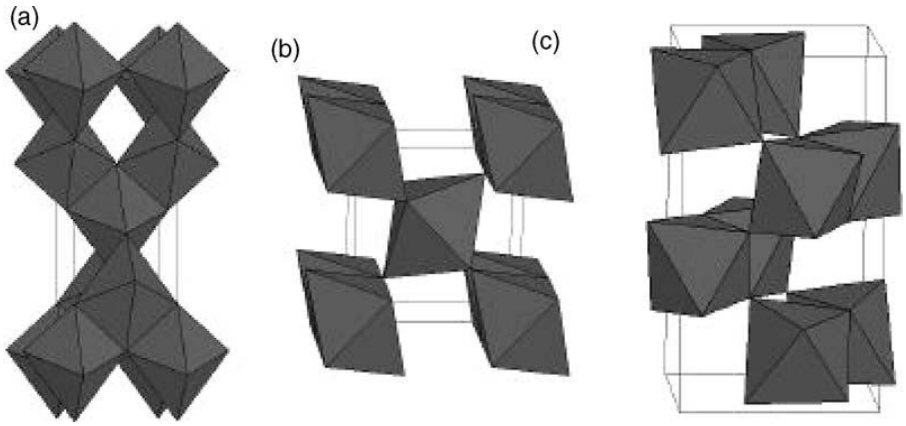

Figure 1.1- Crystal structures of anatase (a) rutile (b) and brookite (c) [9].

The commercial TiO_2 most used in photocatalytic applications is AEROXIDE® P25 which is not pure anatase but a mixture of ca. 80% of anatase and 20% of rutile crystalline phases. The photoefficiency of a certain material is attributed not just to the crystalline phase composition. It must be pointed out that thin films of amorphous TiO_2 have also shown to be photocatalytic active [10]. Other characteristics like particle size are also relevant [11].

Bare TiO_2 is broadly used as photocatalyst. Notwithstanding, its band gap energy of 3.2eV is such high that merely UV light is able to excite the electrons from the VB to the CB to form the e^-/h^+ pairs. Considering that UV light is merely ca. 3-6 % of sun radiation, the band gap energy of TiO_2 appears to be a drawback when the objective is to use the sun light in photocatalytic applications [12]. The development of TiO_2-based catalysts with an overall narrower band gap appears to be an interesting issue, reducing the operating costs of the process by using sun radiation, as it is a natural source of light.

Some previous investigations reported in literature have already demonstrated that TiO_2 composites using carbon materials, such as CNT, have, in fact, visible response in the photocatalytic oxidative degradation of organic pollutants [13-15]. Besides the photosensitizer effect of CNT on CNT/TiO_2 composites, these materials can also act as a

dispersing agent of TiO_2 particles and enhance the specific surface area of the resulting composite.

The mechanism that is believed to operate in a sensitized photoreaction with CNT/TiO_2 composites is partially represented in the schemes of Fig. 1.2a and 1.2b. It must be noticed that the schemes does not show all the reactions involved, but just intends to illustrate the generation of the superoxide (a) and hydroxyl (b) oxidizing agents. The composite catalyst here represented uses Multi-Walled Carbon Nanotubes (MWCNT), instead of SWCNT, but the general idea is the same.

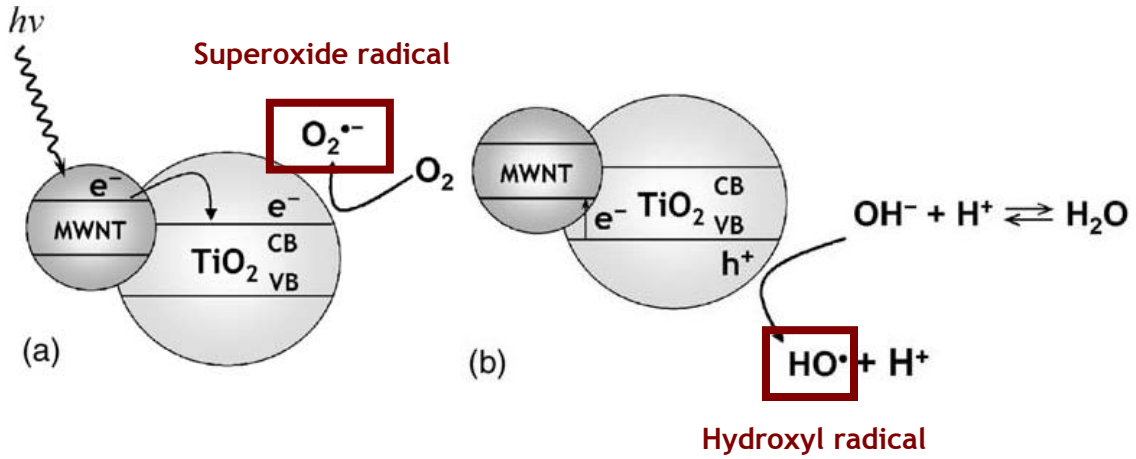

Figure 1.2 - MWCNT acting as photosensitizer in the composite catalyst: (a) following photon absorption, an electron is injected into the CB of TiO_2 semiconductor; (b) the electron is back-transferred to MWCNT with the formation of a hole in the VB of TiO_2 semiconductor and reduction of the so formed hole by adsorbed OH^- (adapted from [13]).

The mechanism begins with the absorption of visible light by CNT and the excited electrons are transferred to the CB of TiO_2. If the diffusion of the e^-/h^+ pairs to the photocatalyst surface is more effective than e^-/h^+ recombination and molecular oxygen present in the reaction medium is abundant, it will be reduced by the excited e^- at the surface of TiO_2 to form the superoxide radical. On the other hand, electrons on the VB of TiO_2 can migrate to the surface of CNT generating positive holes which will oxidize the hydroxide anions to form hydroxyl radicals. The formed oxidizing agents will initiate the photodegradation of organic pollutants.

It is believed that the chemical interaction between CNT and TiO_2, and subsequent photocatalytic activity, depends on the surface chemistry of CNT during the preparation of CNT/TiO_2 composites. In this context, the next section is focused on CNT and their surface chemistry.

1.2 CNT and surface chemistry

CNT are structures of the highest interest due to their unique properties, such as highly mechanical resistance and thermal stability under oxidizing atmosphere conditions [16, 17]. Depending on the way in which the graphene layers are rolled up, CNT have metallic features or electrical semiconductive properties [18]. Since 1991, the investigation on these materials became recurrent with the first steps on the synthesis of MWCNT by Iijima [19]. Single-shell structures were required to finely understand their properties and two years latter, the successful synthesis of SWCNT by Arc-Discharge was reported by both Iijima *et al*. [20] and Bethune *et al*. [21].

Numerous studies have been oriented to the application of CNT as support materials in catalysis, namely in hydrogenation reactions, hydrocarbons decomposition or development of fuel cell electrocatalysts [17]. Several other applications have been reviewed [22] and some examples are energy storage, sensors, conductive and high-strength composites.

Ideal CNT are made of one (SWCNT) or more (MWCNT) graphene sheets with hexagonal display of sp^2 hybridized carbon atoms. However, CNT are not such perfect structures as they were thought to be. Several properties, which were studied for ideal CNT, depending mainly on their diameter and chirality are also hardly affected by the presence of defects such as pentagons, heptagons, vacancies or dopant species [23]. New potential applications are being investigated by introducing defects and modifying the surface chemistry of CNT [24, 25]. Depending on the required application, several chemical agents can be introduced at the surface of CNT like alkali metals [26], salen complexes [27] or amines to form aniline composites [28]. Notwithstanding, since CNT are considered as almost inert substrates, they are previously subjected to oxidizing treatments and, depending on the conditions and the oxidizing agents used, unlike resulting surface chemistry and structural integrity modifications on distinct levels are observed [28-33].

The chemical surface modification of carbon materials using nitric acid (HNO_3) is not a recent issue [34-41]. It has been performed over distinct carbon materials like activated carbons [40, 41], carbon xerogels [42, 43], graphite [44] or ordered mesoporous carbons (OMC) [45, 46]. CNT are often functionalized using oxidative liquid phase treatments with HNO3 [47] to introduce oxygenated functionalities (carboxylic acids, lactones, anhydrides, phenols, carbonyls or quinones) resulting in much higher reactive substrates than pristine CNT.

The introduction of oxygen-containing groups on the surface of CNT enhances their solubility in aqueous or organic solvents and can reduce the van der Waals interactions between distinct CNT, promoting the separation of nanotube bundles into individual tubes. In addition,

HNO_3 is known to be selective on the oxidation of amorphous carbon [48] and can be used as a pre-treatment to provide CNT with a homogeneous surface.

Studies performed over SWCNT, seeking for the effect of chemical oxidation on their structure, show that functionalization by means of HNO_3 causes the opening of the tube caps but basically retain their pristine electronic and mechanical properties. No significant defects are additionally produced, thus the chemical modification mostly occurs at the opened caps and at the already existing defects along the sidewall of SWCNT [25].

HNO_3 treatments have been extensively used at very high concentrations using boiling methods [29], which are very efficient for the introduction of a high density of oxygen-containing groups. Nevertheless, it is worth to say that usually they are not applied in a controlled mode, since correlations between the degree of functionalization and the conditions used are missing. Given the relevance of the functionalization step in the preparation of different carbon based materials for numerous applications, the development of methods for the controlled modification of their surface chemistry is required.

Recently, a new methodology was developed in our group for the controlled functionalization of carbon xerogels based on HNO_3 hydrothermal oxidation [49]. In the present work, the surface functionalization of SWCNT is drawn to tailor the introduction of oxygenated functionalities using the same HNO_3 hydrothermal oxidation procedure. Both type of preferential groups formed and changes on textural properties are assessed under different HNO_3 concentrations (0.01 – 0.3 mol L^{-1}) and at two temperatures (393 and 473 K). A comparison between structural and chemical modifications observed for SWCNT and those presented by Silva *et al.* [49] for carbon xerogels is addressed.

The controlled functionalization of CNT is the primary step for the further preparation and optimization of SWCNT/TiO_2 photocatalysts since the chemical interaction between both materials is expected to be enhanced during the formation of the composite.

2 Experimental

2.1 Functionalization of SWCNT

Pristine SWCNT synthesized by Chemical Vapor Deposition (CVD) were purchased from Shenzhen Nanotechnologies Co. Ltd. (NTP) with the following manufacturer data: purity of CNT > 90%, purity of SWCNT > 50%, main range of diameter < 2 nm, length = 5 – 15 μm, amorphous carbon < 5%, ash content ≤ 2 wt%. The as received material is referred as pristine SWCNT in this work. It is important to note that the sample is mostly constituted by SWCNT but the exact amount of SWCNT is unknown since it was not provided by the manufacturer. The surface chemistry of these SWCNT was modified by introducing different oxygenated functionalities through the HNO_3 hydrothermal oxidation approach.

2.1.1 HNO_3 Hydrothermal Oxidation

The functionalization of SWCNT followed an experimental procedure described elsewhere [49]. Accordingly, a 160 mL autoclave (Parr Instruments, USA Mod. 4564) equipped with a temperature controller and a turbine-type agitation system was used (Fig. 2.1).

Figure 2.1 - Autoclave and temperature controller used in the functionalization of the SWCNT.

75 mL of a HNO_3 solution (concentrations ranging from 0.01 to 0.3 mol L^{-1}) prepared from HNO_3 65 wt % (Fluka) were transferred to the vessel and a certain amount of pristine SWCNT was added (0.2 or 0.5 g). The autoclave was sealed and the solution was flushed with nitrogen for 5 min to ensure removal of dissolved oxygen. The system was further pressurized with

0.5 MPa of N_2, stirred at 300 rpm, and heated until the desired temperature (393 or 473 K) at autogeneous pressure. After 2h of operation, the autoclave was allowed to cool until ambient temperature and then depressurized. The recovered SWCNT were washed several times with distilled water until a neutral pH was attained and dried over night at 393 K. Additionally, a blank test with distilled water instead of the HNO_3 solution was performed.

2.1.2 SWCNT Characterization

Temperature Programmed Desorption (TPD) analysis was carried out using an AMI-200 Catalyst Characterization Instrument (Altamira Instruments) equipped with a quadruple mass spectrometer (Ametek, Mod. Dymaxion). The sample (0.1 g) was placed in a U-shaped quartz tube and heated at 5 K min^{-1} in an electrical furnace under a constant flow of 25 cm^3 min^{-1} (STP) of helium, used as carrier gas. The concentration of CO and CO_2 released was determined using the calibration performed at the end of each analysis.

The amount of volatiles, fixed carbon and ash content was assessed for each sample by Thermogravimetric Analysis (TGA) using a Mettler M3 balance. Firstly, humidity was removed at a constant temperature of 383 K under N_2. Then, the samples were heated at 25 K min^{-1} until reach the temperature of 1173 K. The weight change observed during this stage allows the calculation of the amount of volatile compounds at the surface. When a constant weight was established, the amount of fixed carbon was determined and the gas feed was turned to O_2 until a new stable weight was reached. At these conditions, the entire organic fraction of the sample is burned and the remaining material corresponds to the ash content.

The specific surface area (S_{BET}) of the materials was determined by multipoint analysis of N_2 adsorption isotherms at 77 K in the relative pressure range from 0.05 to 0.3 using BET method, with a Quantachrome NOVA 4200e multi-station apparatus. Each sample was firstly degassed for 6 h at 573 K.

A JEOL 2010F analytical electron microscope, equipped with a Schottky field-emission gun (FEG) was used for high-resolution transmission electron microscopy (HRTEM) investigations. The samples for HRTEM were prepared from the diluted suspension of nanoparticles in ethanol. A drop of suspension was placed on a lacey carbon-coated Ni grid and allowed to dry in air.

2.2 Preparation and characterization of bare TiO_2 and hybrid SWCNT/TiO_2 photocatalysts

The prepared materials to be used in photocatalytic experiments were synthesized by means of a modified sol-gel method. Some of these materials were further subjected to a hydrothermal treatment at 473 K using a 0.1 mol L^{-1} HNO_3 solution.

2.2.1 Acid-catalyzed Sol-Gel Method

The preparation of TiO_2 and SWCNT/TiO_2 composite photocatalysts followed an experimental procedure described elsewhere [50]. The method consists in a modified acid-catalyzed sol-gel method (hereafter referred as SG) using an alkoxide precursor: 0.0125 mol of $Ti(OC_3H_7)_4$ (Aldrich, 97%) was dissolved in 25 mL of ethyl alcohol (Panreac, 99.5%) and the solution was stirred magnetically for 30 min; at this time, 0.2 mL of HNO_3 (Fluka, 65 wt.%) was added. In particular for SWCNT/TiO_2 composites, 2.5 mg of SWCNT were introduced into the $Ti(OC_3H_7)_4$ ethanol solution. The mixture was loosely covered and kept stirring until the homogeneous gel formed. The gel was aged in air for several days. Then the xerogel was crushed into a fine powder and dried at room temperature. The powder was calcined at 673 K in a flow of nitrogen for 2 h to obtain pure anatase crystalline phase. SWCNT were used both as received and functionalized with 0.1 mol L^{-1} of HNO_3. The composites that were synthesized with functionalized SWCNT are labeled as 0.1SW/TiO_2 and SW/TiO_2 is for composites when pristine SWCNT were used.

2.2.2 Hydrothermal Treatment

Some selected materials were subjected to a hydrothermal treatment (hereafter referred as HT) in the same autoclave used to functionalize the SWCNT. One gram of TiO_2 previously prepared by the SG method was introduced into the autoclave together with 2.5 mg of SWCNT. 75 mL of a 0.1 mol L^{-1} HNO_3 solution were transferred to the vessel. The treatment was performed exactly in the same conditions that were applied in the SWCNT functionalization (section 2.2.1). It can be considered that the HT comprised the *in situ* functionalization of the SWCNT with HNO_3. For comparison purposes, a composite was prepared using the commercial AEROXIDE® TiO_2 P25 instead of the TiO_2 prepared by SG, using the same experimental procedure for the hydrothermal treatment. The two different materials are hereafter labeled as SW/TiO_2 – HT and P25/TiO_2.

2.2.3 Photocatalysts Characterization

The diffuse reflectance UV-Vis (DR UV-Vis) spectrum (200 – 800 nm) of all the materials was recorded on a JASCO V-650 UV-Vis spectrophotometer, with a double monochromator, double beam optical system. The spectrophotometer is equipped with an integrating sphere attachment (JASCO ISV-469). The reflectance spectra were converted by the equipment software (JASCO) to equivalent absorption Kubelka–Munk units which are linearly related to the concentration of a diluted sample of infinite tickness (i.e., a sample for each no appreciable changes in spectrum are observed if the thickness is increased). To avoid a decrease on the measured absorbance, the powders were not diluted in any matrix.

The S_{BET} of P25 and the obtained materials prepared both by SG and HT was assessed using the same analytical procedure described in section 2.2.2.

2.3 Photocatalytic Oxidative Degradation of Organic Pollutants

The photocatalytic experiments were conducted in a glass-immersion photochemical reactor equipped with a UV–Vis Heraeus TQ 150 medium pressure mercury vapor lamp located axially and held in a quartz immersion tube and a DURAN 50® glass jacket (Fig. 2.2).

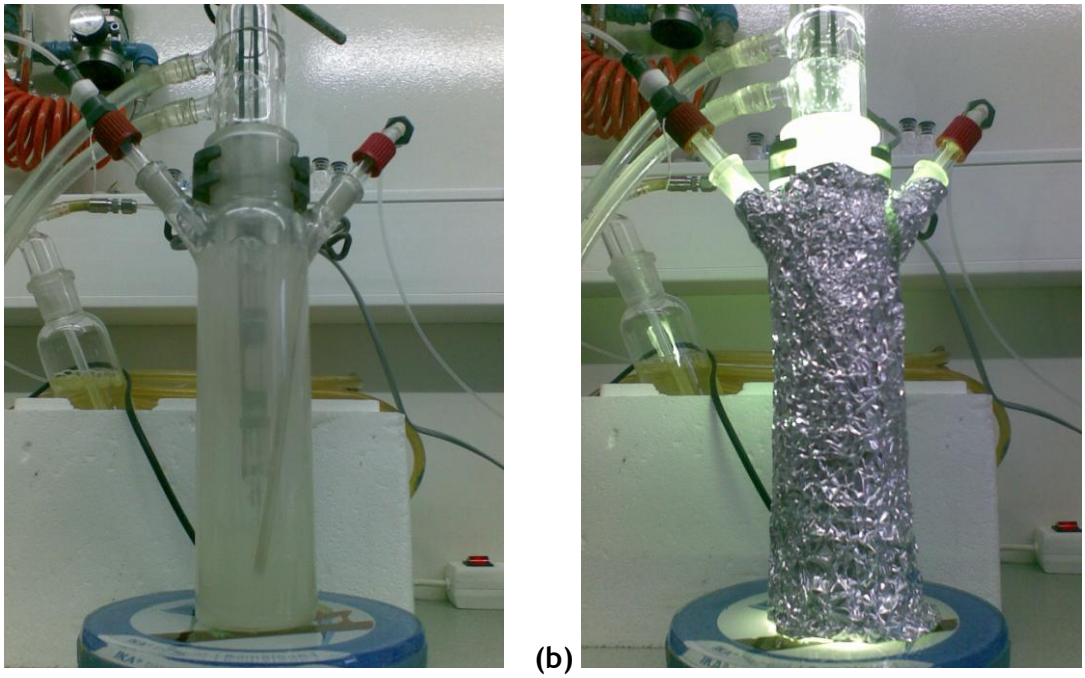

(a) **(b)**

Figure 2.2 - Photoreactor employed on the photocatalytic experiments with the lamp (a) off and (b) on.

The DURAN 50® glass jacket acts as an optical cut-off of UVB and UVC radiation. The main resulting emission lines are 316, 366, 405, 436 nm and above (Fig. 2.3). Inside the glass jacket there was water circulating to cool the irradiation source and cancel the infrared stray radiation, preventing any heating of the suspension.

Two different pollutants were tested for the photocatalytic oxidative degradation: *p*-Methoxyphenol (*p*-MPh) and *p*-Cyanophenol (*p*-CNPh). Substituted phenols are commonly present in many industrial wastewaters including those coming from pesticides, dyes, pharmaceuticals and petrochemical industries. The absorption UV-Vis spectra (250 – 500 nm) of 10 mg L^{-1} solutions of both *p*-MPh and *p*-CNPh were recorded in the same spectrophotometer used in the photocatalysts characterization (section 2.2.3).

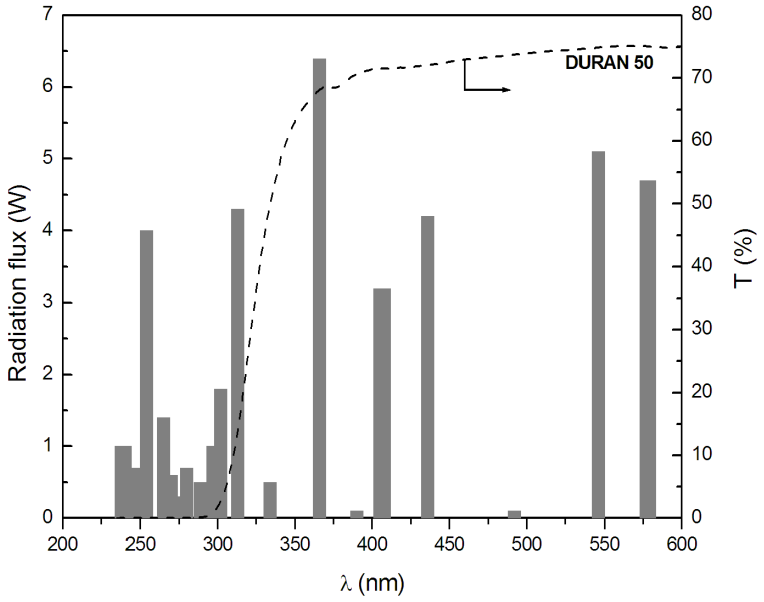

Figure 2.3 - Radiation flux of Heraeus TQ 150 immersion lamp and transmission Spectrum of the DURAN 50® filter (manufacturer data).

A 200 mL min^{-1} oxygen/argon (20 vol.% of oxygen) stream was continuously supplied to the reactor, previously charged with 250 mL of the model pollutant solution (100 mg L^{-1}) and with a fixed amount of TiO_2 in the catalytic tests (1 g L^{-1}). Before turning on the lamp, the suspensions were magnetically stirred for 30 min to establish an adsorption–desorption equilibrium and the reaction was carried out during the next 180 min. Samples were periodically withdrawn and centrifuged prior to analysis to compound conversion, in order to separate any suspended solids.

These samples were then analyzed by High Liquid Performance Chromatography (HPLC) using a Hitachi Elite LaChrom instrument equipped with a Diode Array Detector (L-2450) and a solvent delivery pump (L-2130) at a flow rate of 1 mL min^{-1}. The stationary phase consisted in a Hydrosphere C18 column (250 mm x 4.6 mm, 5 μm particles) with a gradient method. At first, the column was equilibrated with a A:B (70:30) mixture of 20 mmol L^{-1} NaH_2PO_4 at pH=2.8 (A) and acetonitrile (B), followed by a linear gradient run to A:B (30:70) in 13 min and finally with isocratic elution during 2 min.

Total Organic Carbon (TOC) measurements were performed in a Shimadzu TOC-5000 analyzer.

3 Results and Discussion

3.1 Functionalization of SWCNT

A representative HRTEM micrograph of the pristine SWCNT sample is shown in Fig. 3.1. Both SWCNT and MWCNT were observed and it seems that the SWCNT tends to exist as bundles, which is in accordance with what is reported in literature [20].

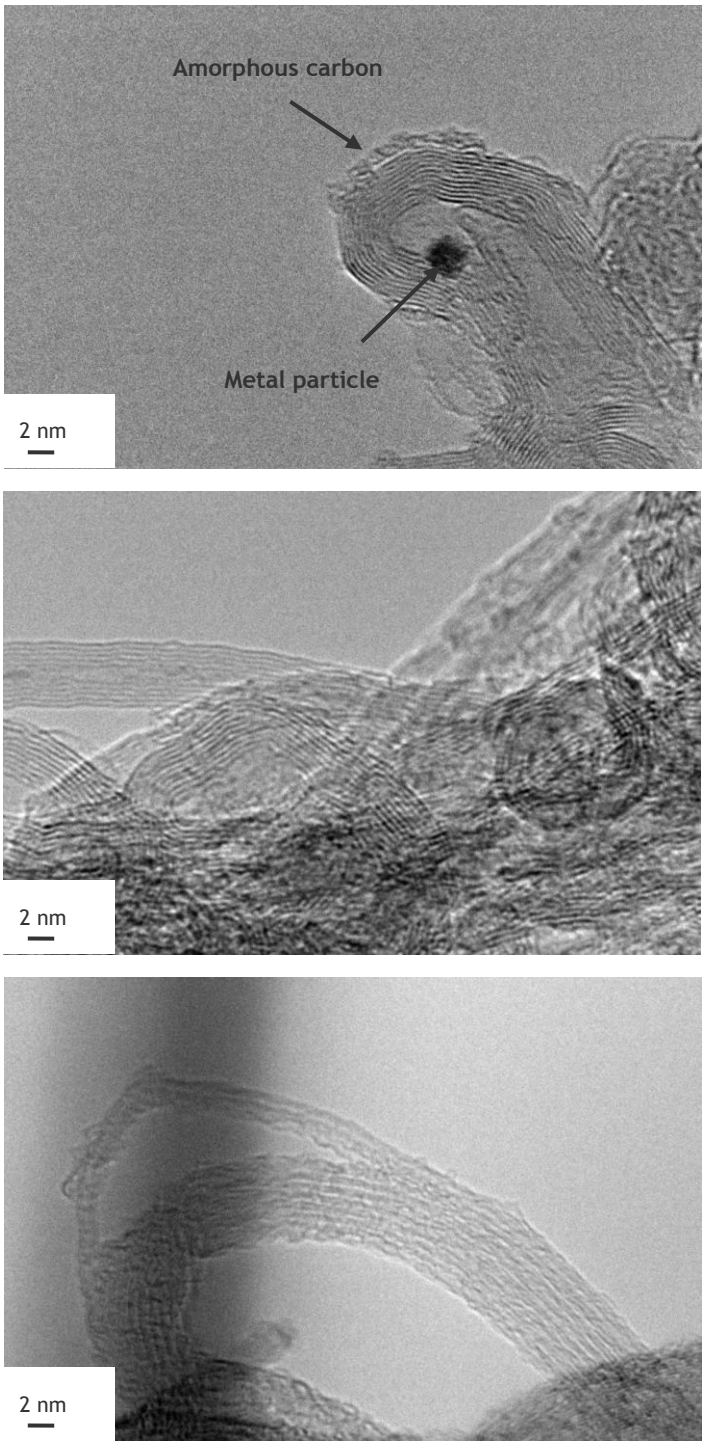

Figure 3.1 - HRTEM micrographs of (a) the pristine SWCNT sample and after treatment with (b) 0.1 mol L^{-1} and (c) 0.3 mol L^{-1} of HNO_3.

Metal particles with ca. 2 nm left from the CNT catalytic synthesis can be observed. The presence of this inorganic material contributes for the ash content of the samples. Also some amorphous carbon is visible at the surface of the nanotubes.

Fig. 3.1b shows a HRTEM micrograph of the sample treated with 0.1mol L^{-1} of HNO_3 at 473 K. In general, HNO_3 treatment seems to clean, to some extent, both amorphous carbon and inorganic material.

Stronger oxidizing conditions affect the structural integrity of these nanotubes, as can be observed in Fig. 3.1c. This is intrinsic of the functionalization process, since oxygenated functionalities can only be introduced if some defects are present over the graphite surface.

Distinct oxygenated groups that are chemically bonded to the surface of CNT, upon oxidizing treatments, can be decomposed upon heating at different temperatures and released as CO or CO_2 [51, 52]. In Fig. 3.2a and 3.2b are represented the TPD spectra corresponding to the groups evolved as CO and CO_2, respectively, from the surface of pristine SWCNT and treated under different HNO_3 concentrations at 473 K.

The amount of oxygenated functionalities introduced on the surface of SWCNT is strongly dependent on the concentration of HNO_3. Comparing the curves obtained for the pristine SWCNT and for the blank test carried out with water instead of HNO_3, it is visible that no considerable amount of groups is present at the surface. This indicates that the introduction of oxygen-containing groups is totally ascribed to the presence of nitric acid instead of some effect of water at high temperatures. By increasing the oxidizing conditions, the amount of groups evolved as CO and CO_2 continuously increases. Both Fig. 3.2a and 3.2b suggest that a good correspondence between the concentration of the oxygenated functionalities and the concentration of HNO_3 exist.

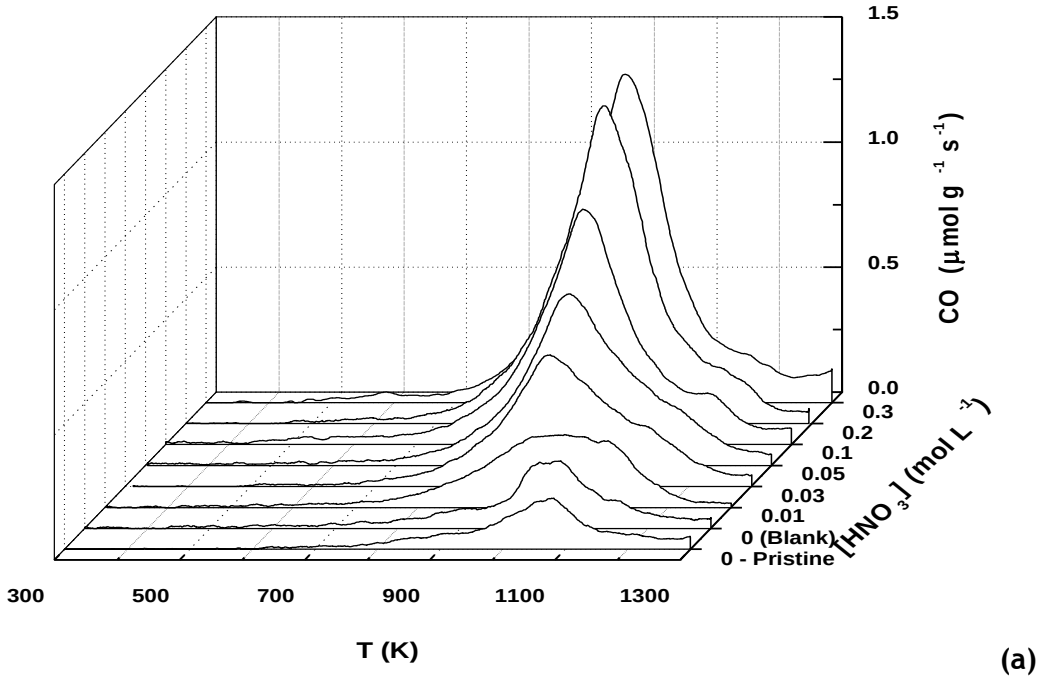

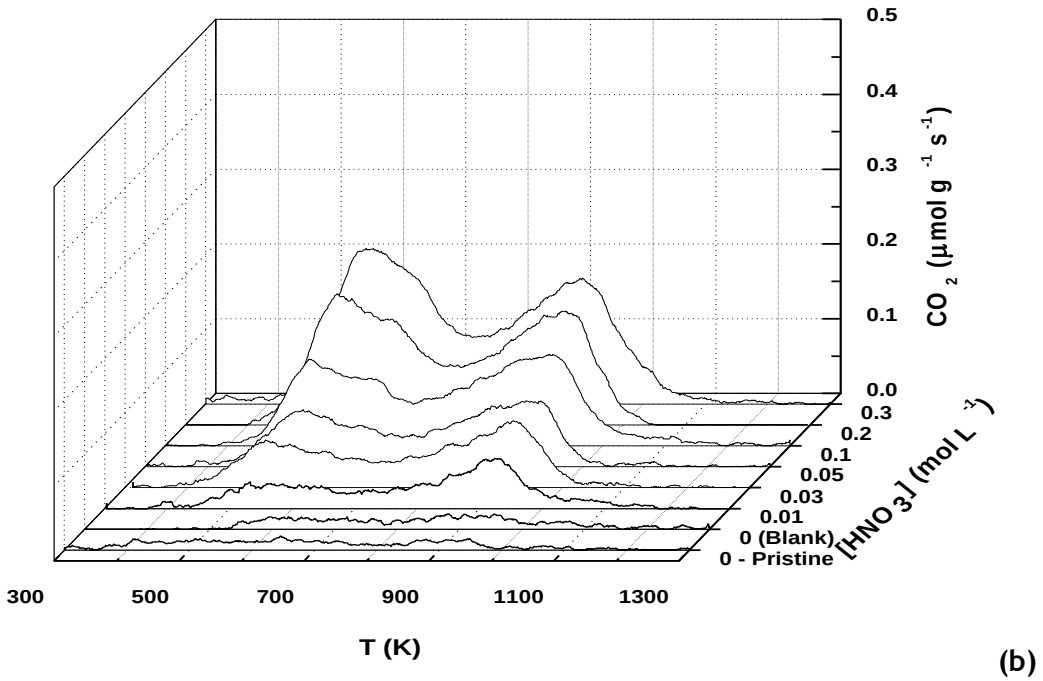

Figure 3.2 - TPD spectra for the pristine SWCNT and treated under different HNO_3 concentrations at 473 K: (a) CO release; (b) CO_2 release.

The measured concentrations of CO and CO_2 for both temperatures tested are gathered on Table 3.1. As previously observed in the TPD spectra, the amount of groups evolved as CO was considerably higher than the one for the moieties evolved as CO_2. Accordingly, the ratio

CO/CO_2 was always higher than unity. This ratio generally decreased while increasing the HNO_3 concentrations.

Table 3.1 - Total amount of CO and CO_2 calculated from the TPD spectra obtained for different HNO_3 concentrations (393 and 473 K).

[HNO_3] (mol L^{-1})	*393 K*			*473 K*		
	CO (±20) (μmol g^{-1})	CO_2 (±20) (μmol g^{-1})	CO/CO_2	CO (±20) (μmol g^{-1})	CO_2 (±20) (μmol g^{-1})	CO/CO_2
Pristine SWCNT	545	90	6.0	545	90	6.0
0 (Blank)	756	75	10.1	714	89	8.1
0.01	661	125	5.3	1034	232	4.5
0.03	---	---	---	1541	350	4.4
0.05	705	109	6.5	1917	388	4.9
0.10	689	120	5.8	2407	586	4.1
0.20	781	173	4.5	3000	724	4.1
0.30	879	158	5.6	3148	907	3.5

To quantify the correlation between the amount of oxygenated groups and the HNO_3 concentration used, the area under the spectrum was plotted against the HNO_3 concentration. In Fig. 3.3 are represented the two curves obtained for CO and CO_2. In addition, in order to test the influence of temperature on the functionalization process, the range of HNO_3 concentrations used at 473 K was also tested over pristine SWCNT at 393 K and the results are shown in the same figure.

It becomes clear that the functionalization degree is not only dependent on the HNO_3 concentration but also on the temperature used. Surface groups are not introduced on SWCNT at 393 K even at the highest HNO_3 concentrations tested. The present results suggest that an activation energy is involved in this method, requiring a certain temperature to initiate the functionalization process. For the temperature of 473 K, the experimental data are quite well adjusted to a single exponential function, as shown in Fig. 3.3.

Comparing the results obtained in this work with those previously obtained in our group for a carbon xerogel using the same functionalization method [49], a similar behaviour is observed, suggesting that an activation energy must be truly associated with the functionalization process. In that study a maximum functionalization degree is attained for 393 K but, when increasing the temperature for 473 K, the concentration of oxygenated functionalities introduced on the surface of the carbon xerogel also increases and no plateau was observed for the highest HNO_3 concentrations.

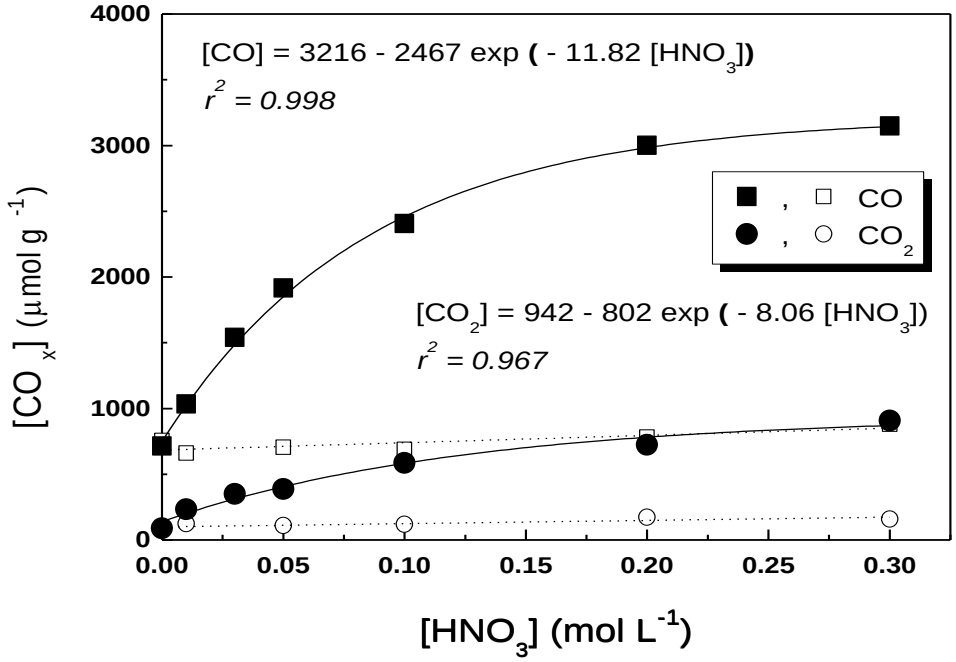

Figure 3.3 - Evolution of the amount of CO and CO_2 with HNO_3 concentration: open symbols – 393 K; full symbols – 473 K (mathematical correlations: $[HNO_3]$ must be inserted in mol L^{-1} for a $[CO_x]$ in μmol g^{-1}).

The amount of oxygen-containing groups introduced on the surface of carbon xerogels was higher than that attained with the SWCNT using the same temperature and HNO_3 concentrations. The difference at the same oxidizing conditions was not constant in the whole range of the HNO_3 concentration, increasing as the HNO_3 concentration increases. This trend seems to be intrinsically related with the distinct morphology of both carbon materials. It is noteworthy that the concept of porosity is quite different when considering carbon xerogels or carbon nanotubes. Carbon xerogels present a type of porosity similar to that of well known activated carbons. The available area for the introduction of the oxygenated functionalities is on the micro, meso and macropores. The porosity of CNT is usually associated to a bundle and not to a single carbon nanotube, since the graphite layers are non porous. The porosity of a bundle of CNT is the result of different contributions [47]: i) the area available at the surface of the bundle, ii) the existing area between distinct individual carbon nanotubes, which is called intersticial and iii) the area inside the pores of the bundle, which corresponds to the inner cavities of the opened CNT. The degree of functionalization must be then always compared taking into account the specific structure of each material.

The BET surface area of pristine and treated SWCNT at 473 K was measured. Pristine SWCNT has a S_{BET} of 370 m^2/g (± 5 m^2/g) and the HNO_3 hydrothermal treatment, as expected, slightly

increased the surface area to near by 400 m^2/g ($\pm$ 5 m^2/g). Acidic treatments are known to open the end caps of CNT, which can contribute for the small raise in S_{BET} (ca. 8 %).

However, when the acidic treatment was carried out over carbon xerogels, the area increased about 30% when high HNO_3 concentrations were used and this was ascribed to the development of the microporosity during the functionalization process [49]. In the case of the carbon xerogel, the introduction of the oxygen-containing groups took place over all the available surface area, whereas for CNT the defects created at the surface of the graphite layers are the single positions which present some chemical reactivity to form the desired functionalities. Therefore, the nature of carbon material should be taken into account when predicting the functionalization degree to be achieved with the HNO_3 hydrothermal treatment, since the morphology seems to be influent on the pathway and the yield of this chemical process.

Considering the temperatures at which different groups are evolved as CO and CO_2 upon heating, the concentration of each group can be determined by deconvolution of TPD spectra [51, 52]. As example, in Fig. 3.4a and 3.4b are represented the deconvolution of the curves of CO_2 and CO, respectively, obtained for the oxidation at 473 K using 0.3 mol L^{-1} of HNO_3.

The distinct oxygenated functionalities are identified by the temperature at which they are released. It is relevant to point out that for the deconvolution process some assumptions were made accordingly to a method reported in literature [52]. For instance, carboxylic anhydrides are supposed to decompose both as CO and CO_2. Once fixed the temperature at which these groups were released as CO_2, the correspondent peak on CO spectrum was defined. The concentration of each group is determined by calculating the area of the correspondent peak.

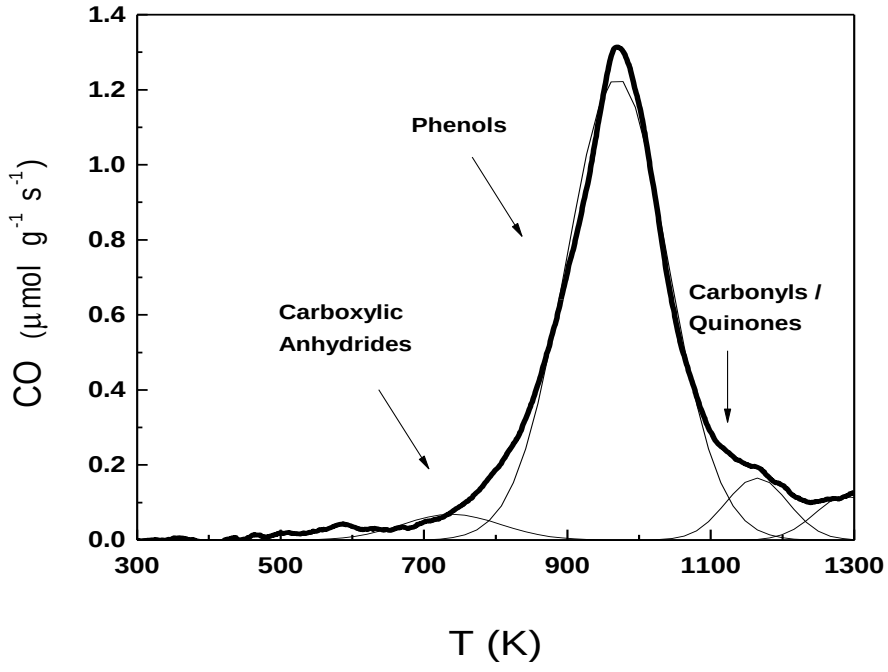

(a)

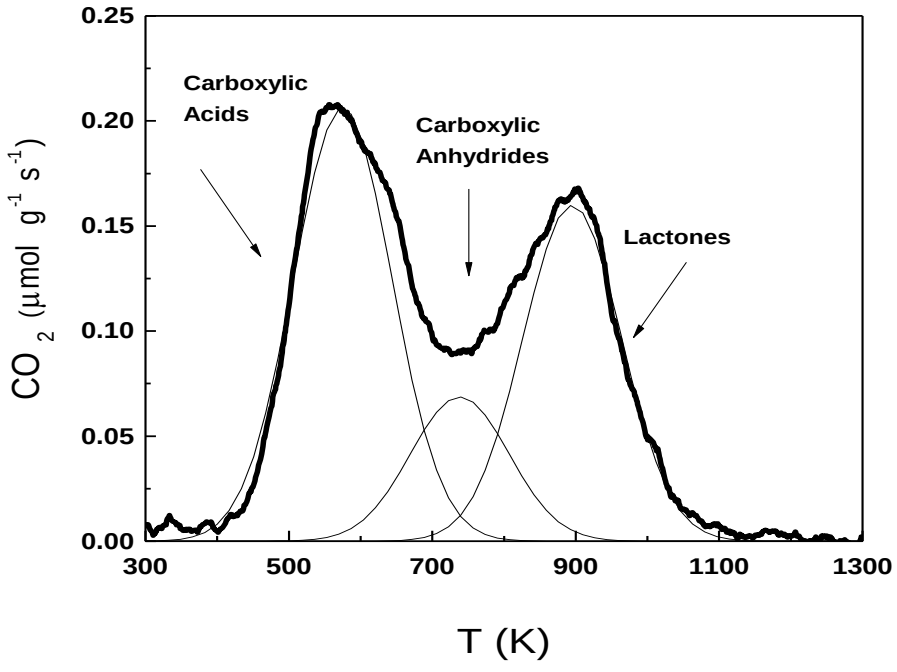

(b)

Figure 3.4 - Deconvolution of TPD spectra for the SWCNT treated with 0.3 mol L^{-1} of HNO_3 at 473 K: (a) CO spectrum; (b) CO_2 spectrum.

The main groups identified on CO_2 spectrum were carboxylic acids and lactones. The oxygenated moieties observed at the highest concentrations on the surface of SWCNT were phenols, as revealed by the CO spectrum. Also carbonyls or quinones were identified, but in lower amounts. All the spectra curves were deconvoluted using the same approach and the

concentrations of each moiety, released as CO and CO_2, is respectively represented as a function of the HNO_3 concentration in Fig. 3.5a and 3.5b.

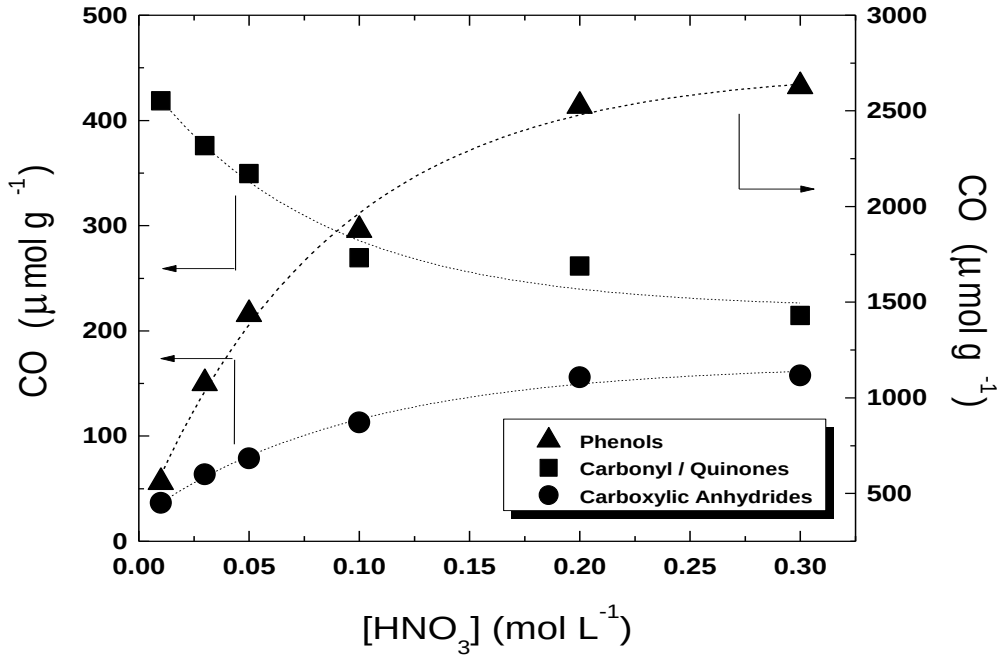

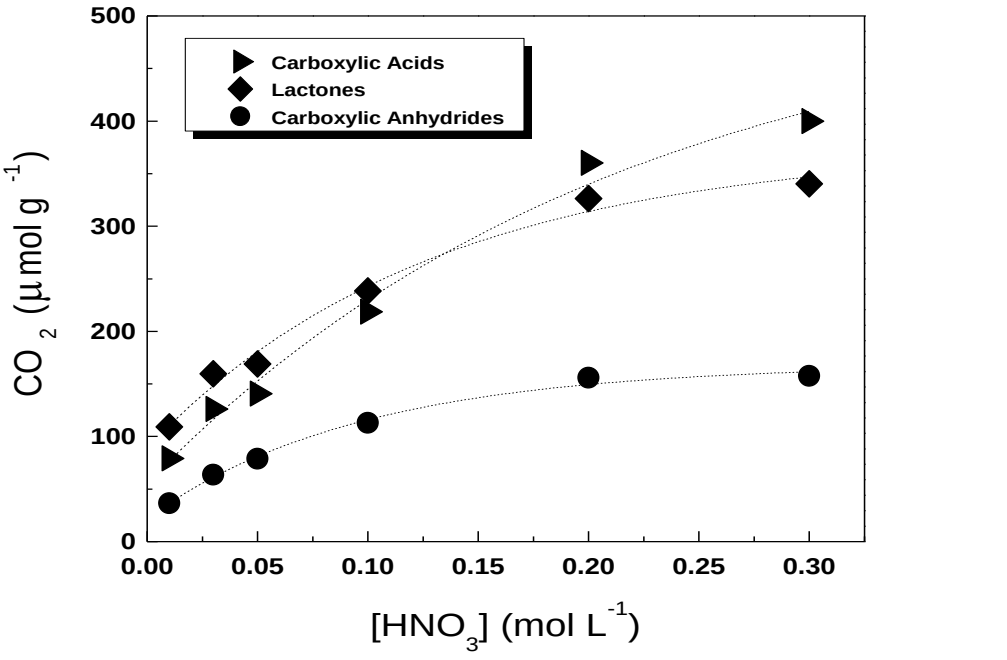

Figure 3.5 - Evolution of the concentration of specific oxygenated groups created at the surface of SWCNT under HNO_3 treatment at 473 K, released as (a) CO and (b) CO_2.

As found for the total amount of groups at the surface of SWCNT, an exponential function also fits the results obtained for the concentration of each single oxygenated moiety. It is relevant to note that the concentration of all functionalities increase with HNO_3 concentration except for the carbonyl/quinones groups. The mechanism proposed in the literature reports that the formation of oxygen-containing surface groups seems to follow a progressive pathway starting with the creation of phenols (-OH) and carbonyl/quinones (C=O) being further developed into carboxylic functionalities (-COOH) if the material is exposed to oxidizing conditions for enough time to allow their formation [48, 53, 54]. Under our oxidizing conditions, the development of phenols is obvious but their conversion into other functionalities is not clear. However, the formation of carboxylic groups seems to be a consequence of the carbonyl/quinones firstly created at the surface of the SWCNT.

The weight percentage of the total amount of molecular oxygen released (% O_2) as CO and CO_2 was calculated based on the concentrations determined by TPD analysis. The results are gathered in Table 3.2 for both temperatures tested (393 and 473 K) and represented in Fig. 3.6 for the temperature of 473 K.

Table 3.2 - Quantification of volatiles, ash content (determined by TGA) and %O_2 (determined by TPD) for the SWCNT treated at different HNO_3 concentrations (393 and 473 K).

[HNO_3] (mol L^{-1})	*393 K*			*473 K*		
	% O_2 (wt. %)	% Volatiles	% Ash Content	% O_2 (wt. %)	% Volatiles	% Ash Content
Pristine SWCNT	1.2	7.0	6.9	1.2	7.0	6.9
0 (blank)	1.4	10.2	6.6	1.4	9.3	8.6
0.01	1.5	10.0	6.1	2.4	10.2	5.5
0.03	---	---	---	3.6	12.3	4.5
0.05	1.5	9.3	7.0	4.3	13.3	3.1
0.10	1.5	12.1	6.3	5.7	15.8	3.3
0.20	1.8	---	---	7.1	18.5	3.1
0.30	1.9	12.9	6.3	7.9	19.2	3.4

The total amount of molecular O_2 is representative of the total concentration of oxygenated groups introduced on the surface of SWCNT. As expected, the trend of the O_2 released corroborates the TPD results. For the temperature of 393 K, no considerable surface modification was observed. Contrarily, at 473 K, the total amount of oxygenated groups increases progressively with the HNO_3 concentration. Despite the poor surface chemistry of pristine SWCNT with an O_2 concentration of 1.2 wt. %, the HNO_3 hydrothermal treatment is

able to provoke a considerable surface modification, introducing 7.9 wt. % of molecular O_2 at the strongest oxidizing conditions tested (0.3 mol L^{-1} of HNO_3).

Weight % of volatiles and ash content was determined by TGA (Table 3.2). The temperature of 393 K is not sufficient neither to modify the surface of CNT nor to remove the ash content present in the material. Since volatiles correspond mainly to the oxygenated functionalities that are released during TGA, the results at 473 K are once again fitted to a single exponential function and follow the same trend as found for the evolution of molecular oxygen (Fig. 3.6). The difference observed between the amount of volatiles and the molecular oxygen can be related to some nitrogen functionalities that contribute to the weight loss during TGA but are not measured as CO or as CO_2 during TPD analysis. At variance to what happened at 393 K, the HNO_3 treatment at 473 K was able to remove up to 50% of the ash content of pristine SWCNT (Table 3.2). The ash content decreased from 6.9% for the original material to around 3.1-3.4 % for SWCNT treated with HNO_3 concentrations above 0.05 mol L^{-1}, in agreement with the previous HRTEM observations. Therefore, temperature and HNO_3 concentration are key parameters for the activation of the functionalization process as well as for the removal of the inorganic material that remains in the samples from the synthesis of SWCNT, which are produced by CVD.

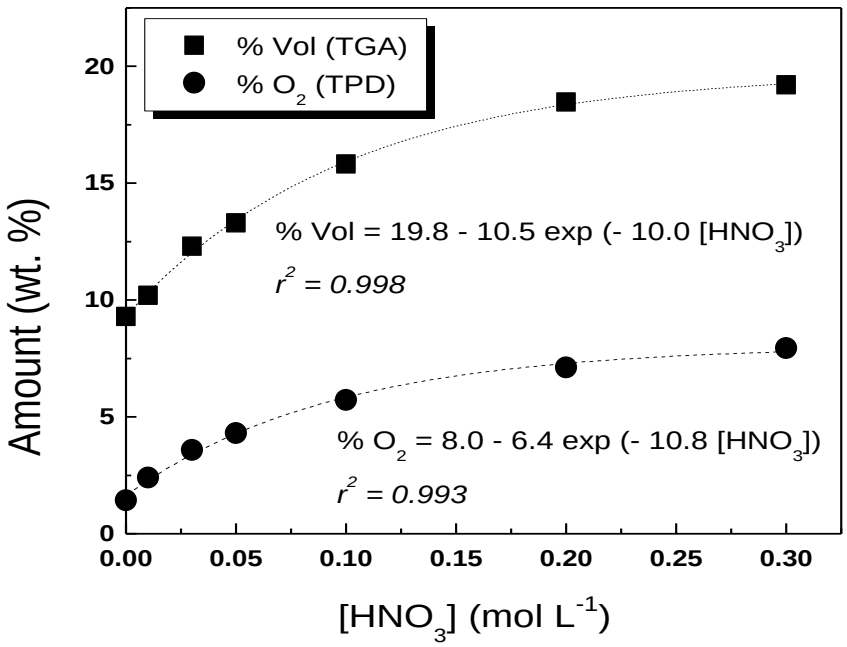

Figure 3.6 - Amount of volatiles (determined by TGA) and molecular O_2 (determined base on TPD spectra) present at the surface of SWCNT treated with different HNO_3 concentrations at 473 K (mathematical correlations: [HNO_3] must be inserted in mol L^{-1}).

When comparing the functionalization of SWCNT with carbon xerogels using the same method and experimental conditions, it is noticeable that the functionalization degree in terms of % O_2 is about 2.5 times higher for carbon xerogels (at a concentration of 0.3 mol L^{-1} HNO_3). As previously discussed, the difference observed may be ascribed to the structural properties of the materials. CNT are very well organized carbon materials with perfect graphite layers and thus poor reactive due to the high chemical stability. In this case, the introduction of oxygenated functionalities proceeds over the defects that are introduced during HNO_3 hydrothermal treatment. On the other hand, carbon xerogels are structures with a totally distinct morphology, like a bulk material with a developed porosity. In this case, the carbon structure is not so perfectly organized like in CNT, thus providing more sites for the attachment of the oxygenated moieties. Therefore, the reactivity of carbon xerogels is supposed to be much higher than the one of CNT, which can explain the difference on the functionalization degrees achieved with the current HNO_3 hydrothermal treatment. However, in both cases, the % O_2 is correlated with the HNO_3 concentration by an exponential function as presented for SWCNT in Fig. 3.6.

During each HNO_3 hydrothermal run, it was verified that the SWCNT weight loss (WL) varied significantly with the conditions used. WL means the difference between the weight of SWCNT introduced into the autoclave (0.2 g, in this case) and the final weight of the recovered material after the HNO_3 hydrothermal treatment, given in percentage. In Fig. 3.7 is represented the WL observed as a function of HNO_3 concentration for both 393 and 473 K.

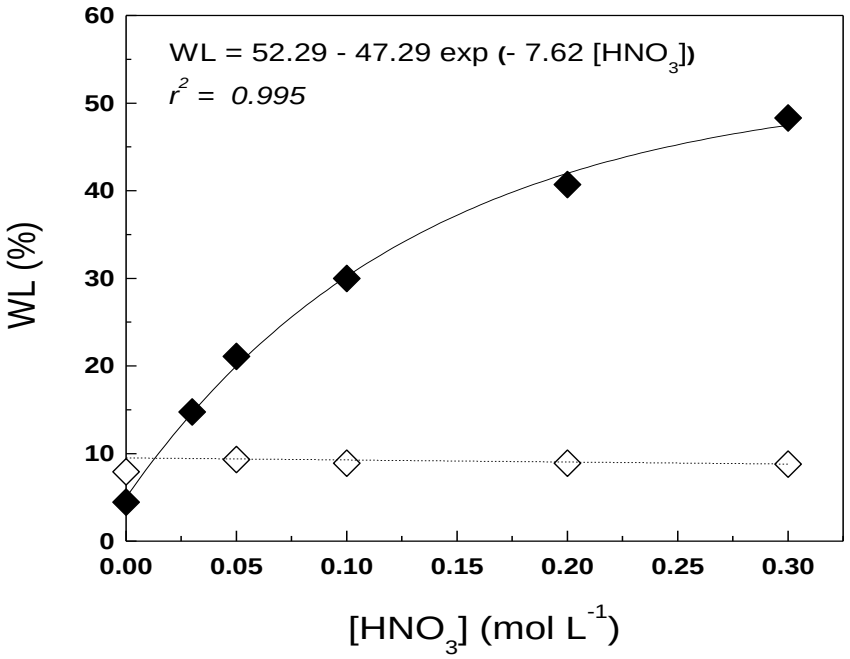

Figure 3.7 - WL observed after the HNO_3 treatment at different concentrations: open symbols – 398 K; full symbols – 473 K (mathematical correlations: [HNO_3] must be inserted in mol L^{-1}).

For the temperature of 393 K, the WL observed with the increase of the HNO_3 concentration is negligible. However, at 473 K the oxidizing conditions are such that the WL varies significantly with the used HNO_3 concentration (5-50 %). As observed for the amount of oxygenated functionalities introduced in the surface of SWCNT, an exponential function fits the WL experimental data, suggesting that both phenomena are correlated. In fact, during acidic oxidation process, CNT can collapse and form carbonaceous fragments (CFs). It is reported that the carboxylated functions produced by HNO_3 treatment are mainly on carboxylated carbonaceous fragments (CCFs) adsorbed on SWCNT instead of directly covalently anchored to the surface of SWCNT [55]. Under strong enough oxidizing conditions these CCFs can be fully gasified to form CO_2, which can explain the verified WL.

However, in the case of the carbon xerogel, the reported WL during the same HNO_3 hydrothermal treatment did not exceed 10% under the same conditions [49]. Since the WL of the SWCNT verified during the blank test (with water instead of HNO_3) was in the range of the measured values for the carbon xerogel (5-10 %), it is believed that the mechanism undergone by both materials during the exposure to the HNO_3 oxidizing conditions for this same HNO_3 hydrothermal process is truly different. Therefore, there are many aspects in the HNO_3 hydrothermal treatment that influence the mechanism and the yield of oxygenated functionalities introduced over their surface. Reaction temperature and HNO_3 concentrations are the key operation conditions to tune the functionalization of these carbon materials. In addition, when choosing a carbon material for a certain application which requires previous surface functionalization, the morphology is also a relevant issue since the reaction pathway appears to go in different ways.

Additionally, some tests were performed by loading the reactor with 0.5 g of SWCNT instead of 0.2 g and using three different HNO_3 concentrations (0.03, 0.1 and 0.3 mol L^{-1}). The CO and CO_2 concentrations are gathered in Table 3.3, as well as the % O_2, and the respective TPD spectra presented in Fig. 3.8.

Table 3.3 - Total amount of CO and CO_2 calculated from the TPD spectra and respective % O_2 as function of $[HNO_3]/m_{SWCNT}$ and HNO_3 concentration at 473 K.

$[HNO_3]$ (mol L^{-1})	*m_{SWCNT} (g)*	*$[HNO_3]$ / m_{SWCNT} (mol L^{-1} g^{-1})*	*CO (±20) (μmol g^{-1})*	CO_2 (±20) (μmol g^{-1})	CO/CO_2	% O_2 (wt. %)
0.03	0.5	0.06	1134	184	6.2	2.4
0.03	0.2	0.15	1541	350	4.4	3.7
0.10	0.5	0.20	1888	428	4.4	4.4
0.10	0.2	0.50	2407	586	4.1	5.9
0.30	0.5	0.60	2535	606	4.2	6.2
0.30	0.2	1.50	3148	907	3.5	8.4

As expected, for the groups released as CO (Fig. 3.8a) and for the groups released as CO_2 (Fig. 3.8b), the amount of surface groups obtained with the same HNO_3 concentration is always lower for the load of 0.5 g.

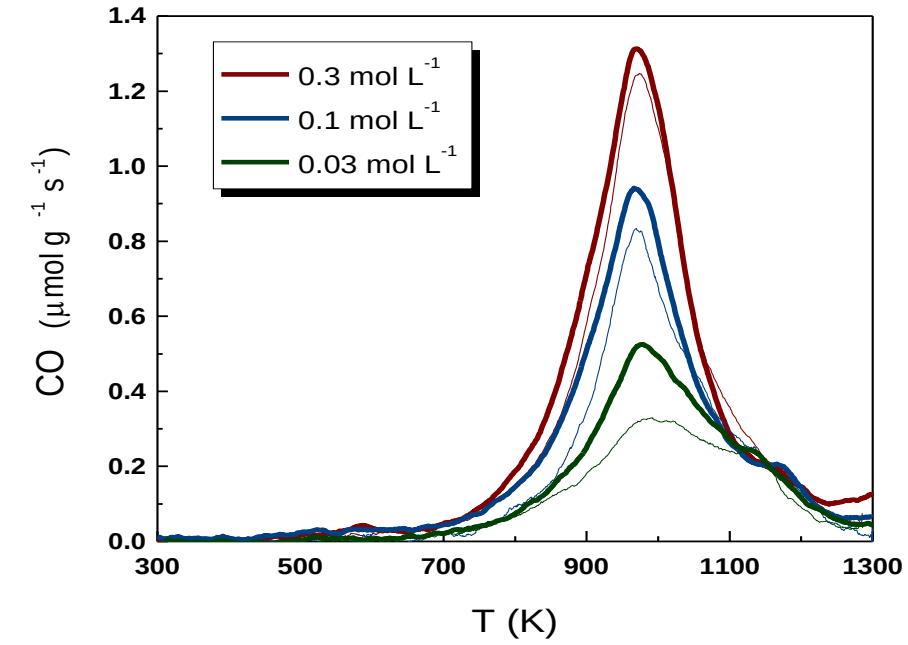

(a)

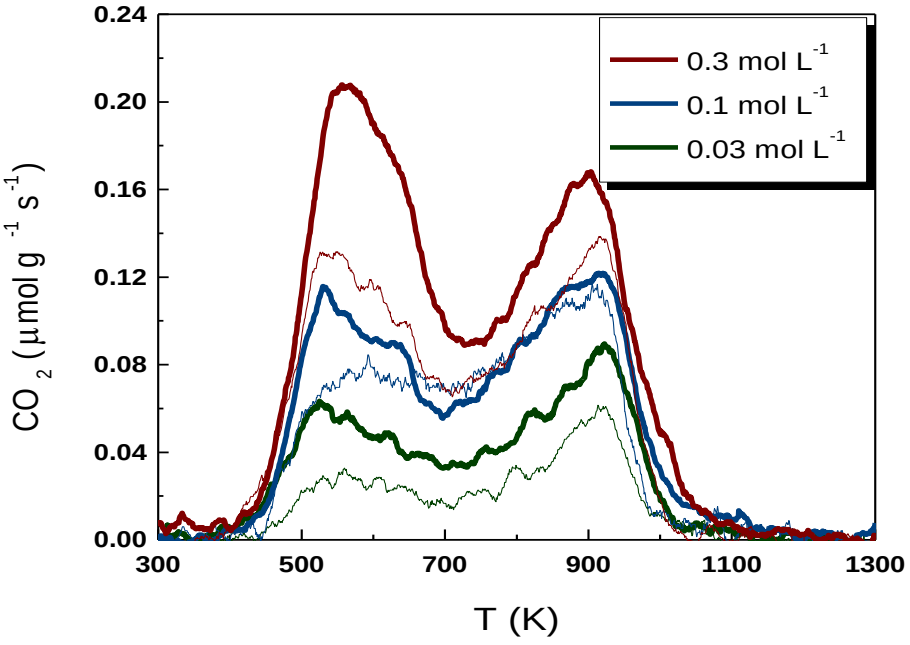

(b)

Figure 3.8 - TPD spectra for different SWCNT loads and treated at three different HNO_3 concentrations: bold lines – 0.2g; non bold lines – 0.5g. Release of (a) CO and (b) CO_2.

In Fig. 3.9 is plotted the percentage of the total amount of molecular oxygen determined by TPD (released as CO and CO_2) against $[HNO_3]/m_{SWCNT}$ for all the SWCNT loads and HNO_3 concentrations studied at 473 K.

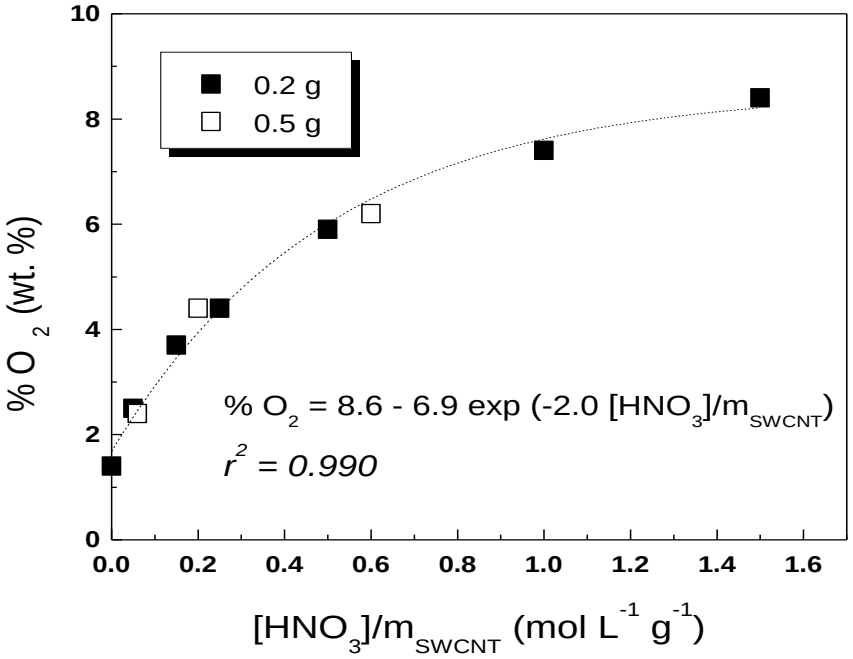

Figure 3.9 - Weight % O_2 determined by TPD for the SWCNT treated at 473 K as a function of $[HNO_3]/m_{SWCNT}$ (mathematical correlation: $[HNO_3]$ must be inserted in mol L^{-1}).

As expected, the % O_2 is dependent on the $[HNO_3]/m_{SWCNT}$ ratio. In addition, since one single mathematical correlation represents quite well the data for both loads (0.2 g and 0.5 g), for a given $[HNO_3]/m_{SWCNT}$ ratio the % O_2 seems to be independent with respect to the SWCNT load (i.e. when the HNO_3 concentration increases proportionally to the SWCNT load in order to maintain the $[HNO_3]/m_{SWCNT}$ ratio).

Therefore, a mathematical correlation between the amount of oxygenated groups which can be introduced at the surface of SWCNT and the $[HNO_3]/m_{SWCNT}$ ratio is established. The functionalization degree can now be predicted not also for a fixed load of SWCNT but for the whole range of $[HNO_3]/m_{SWCNT}$ studied, including several SWCNT loads and HNO_3 concentrations. The surface modification of SWCNT by the HNO_3 hydrothermal method can be accurately controlled by using the mathematical correlations obtained.

3.2 Characterization of hybrid SWCNT/TiO_2 photocatalysts

The SWCNT functionalized with 0.1 mol L^{-1} of HNO_3 were used to prepare one composite by the SG method (0.1SW/TiO_2).

DR UV-Vis spectra of the materials prepared by SG (TiO_2, SW/TiO_2 and 0.1SW/TiO_2) and those submitted to a HT (SW/TiO_2 – HT and P25/TiO_2 - HT) are represented in Fig. 3.10. The spectrum obtained for the commercial P25 is also shown and TiO_2 is considered as the reference material for comparison purposes.

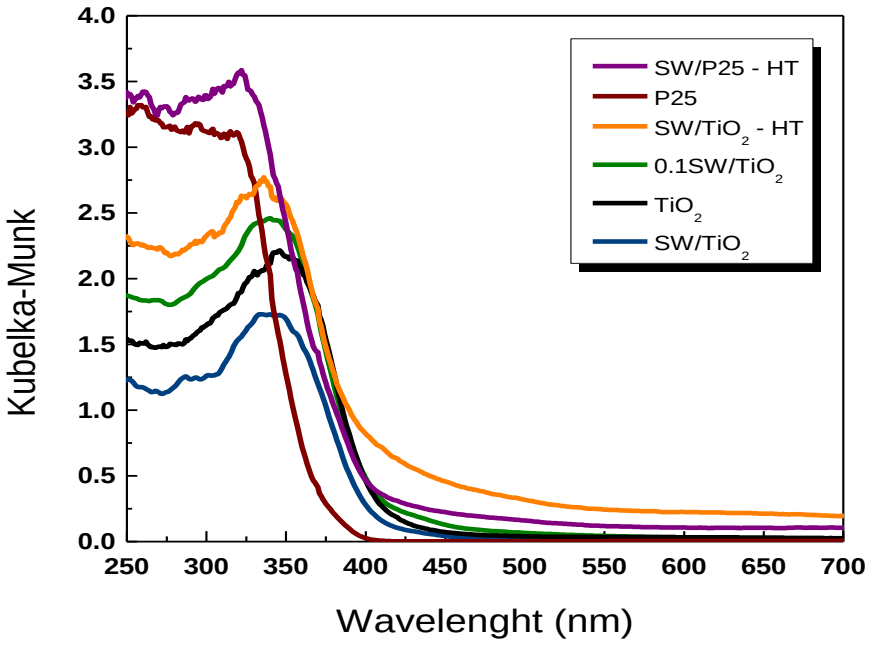

Figure 3.10 - Diffused reflectance UV-Vis spectra of the different catalysts.

Comparing the materials synthesized by SG, it is clear that no visible absorption was increased with the incorporation of the CNT in the TiO_2 matrix. It is worth to note that, despite CNT are black bodies, the amount of SWCNT in SWCNT/TiO_2 composites used in this work is quite low. Hence, the wavelengths at which the composites absorb are very similar to the ones for the TiO_2 spectrum. Nevertheless, different absorptions were observed. It seems that composites with functionalized SWCNT are able to absorb higher amounts of light in the UV range.

Higher absorptions were also observed for the materials which were subjected to the hydrothermal treatment. In this case, an improvement on visible light absorption was recorded for SW/TiO_2 – HT and for SW/P25 – HT.

Taking into account that in a photocatalytic process the degradation of the substrate takes place at the surface of the catalyst, the specific surface area can be a relevant parameter and must be considered to evaluate the performance of a photocatalyst. The S_{BET} of each specific prepared material was assessed and the results are gathered in Table 3.4.

Table 3.4 - Specific surface area (S_{BET}) determined for the prepared materials and for P25.

Catalyst	TiO_2	SW/TiO_2	SW/TiO_2 - HT	SW/P25 - HT	P25
S_{BET} (m^2/g)	102	74	122	49	47

The incorporation of SWCNT in the TiO_2 matrix produced a decrease in the S_{BET} of about 25%, contrarily to what was expected. The introduction of CNT in a TiO_2 matrix is supposed to produce a better dispersion of the TiO_2 crystallites, increasing the S_{BET}. A possible explanation is that, in the dry step, the gel could collapse in some way reducing the porosity of the material. Further X-Ray Diffraction (XRD) analyses should be performed to clarify this issue.

On the other hand, the HT increased by 25% the S_{BET} of SW/TiO_2 – HT when compared to the material present in the higher amount (TiO_2). The HT of TiO_2 powders is known to affects the particle size, the surface area and the hydroxyl content of the material [56, 57], depending on the treatment conditions. In the present case, the HT was performed with HNO_3 which comprises the *in situ* functionalization of the SWCNT. Hence, the dispersion of the particle size of TiO_2 crystallites could be enhanced resulting in a higher S_{BET}. In the case of P25, no significant differences were observed.

3.3 Photocatalytic Oxidative Degradation of Organic Pollutants

The performance of the prepared materials on the photocatalytic oxidative degradation of two substituted phenolic compounds under UV-Vis irradiation was followed by HPLC and TOC measurements. Different materials were tested for each model pollutant.

3.3.1 Heterogeneous photocatalysis of *p*-Methoxyphenol aqueous solutions

The concentration profiles obtained for the photocatalytic oxidative degradation of *p*-MPh using different catalysts are shown in Fig. 3.11 in terms of C/C_0. Firstly, it must be pointed out that the blank experiment performed in the absence of a catalyst revealed that the probe molecule absorbed the irradiated light being degraded in an extent of around 65 %. Thus, the trends observed for the catalytic tests are the result of two contributions: the catalyst photoefficiency and the degradation of *p*-MPh by the absorption of light. As previously explained in Section 1.1, the oxidative degradation occurred through a catalytic photoreaction, since the light was firstly absorbed by the substrate molecule instead of being firstly absorbed by the catalysts (sensitized photoreaction).

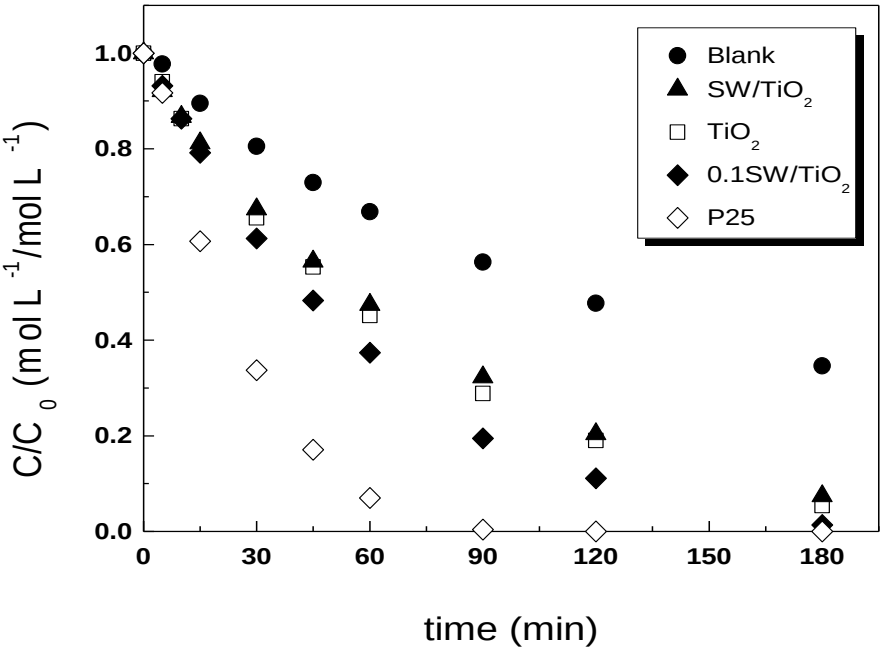

Figure 3.11 - Dimensionless concentration profiles of *p*-MPh during photocatalytic oxidation reactions using different catalysts.

Considering the prepared TiO_2 as the reference catalyst, there was no visible increase on the photodegradation of *p*-MPh when incorporating the SWCNT in the TiO_2 matrix, which is in agreement with the lower S_{BET} measurement and the obtained DR UV-Vis spectrum. Nevertheless, a slight increase was visible when using the 0.1SW/TiO_2 composite. This can possibly be explained by a higher chemical interaction between the CNT and TiO_2, promoting a better dispersion of the crystallites and helping on the migration of the excited electrons from the CNT to the TiO_2 phase. A higher S_{BET} was expected for this material, when compared to TiO_2 and SW/TiO_2. The obtained DR UV-Vis spectrum also corroborates the oxidative results, since higher absorptions were recorded.

However, the best catalyst tested on the oxidative degradation of *p*-MPh was undoubtedly P25 despite its two times lower S_{BET}, when compared with TiO_2. Additionally, it can also be considered that for the range of 300-350 nm P25 absorbs more light than any of the other catalysts tested.

TOC measurements of the collected samples after 180 min of reaction were also assessed in order to evaluate the mineralization degree of the probe molecule. In Table 3.5 are gathered the results obtained for the TOC and pollutant conversions for each photocatalytic experiment. The pH of the final solution was similar for all the experiments (4.0 $\pm$ 0.5) and slightly lower than the pH of the mother solution (5.6).

Table 3.5 - TOC and *p*-MPh conversions at the end of irradiation (180 min).

Catalyst	Blank	SW/TiO_2	TiO_2	$0.1SW/TiO_2$
X_{TOC} (%)	17	40	42	49
$X_{p\text{-MPh}}$ (%)	65	93	95	99

The TOC conversion was significantly lower than the conversion of the pollutant, which indicates that high amounts of photoproducts were still present on the solution and not mineralized. An increase in TOC conversion was observed with the $0.1SW/TiO_2$ composite, when compared with bare TiO_2 and SW/TiO_2. Despite the higher reaction rate observed for P25, almost total conversions could be obtained with the prepared materials at the 180 min of reaction.

Since the objective of the study is to search for the best catalyst for the photocatalytic oxidative degradation of organic pollutants, the proper conditions are those of sensitized photoreaction systems. Hence, further studies were performed with another model pollutant, *p*-Cyanophenol (*p*-CNPh), since the photodegradation of *p*-MPh did not follow a pure sensitized photoreaction due to the absorption of light by this probe molecule (300 – 325 nm). Fig 3.12 shows the absorption UV-Vis spectra of 10 mg L^{-1} solutions of *p*-MPh and *p*-CNPh.

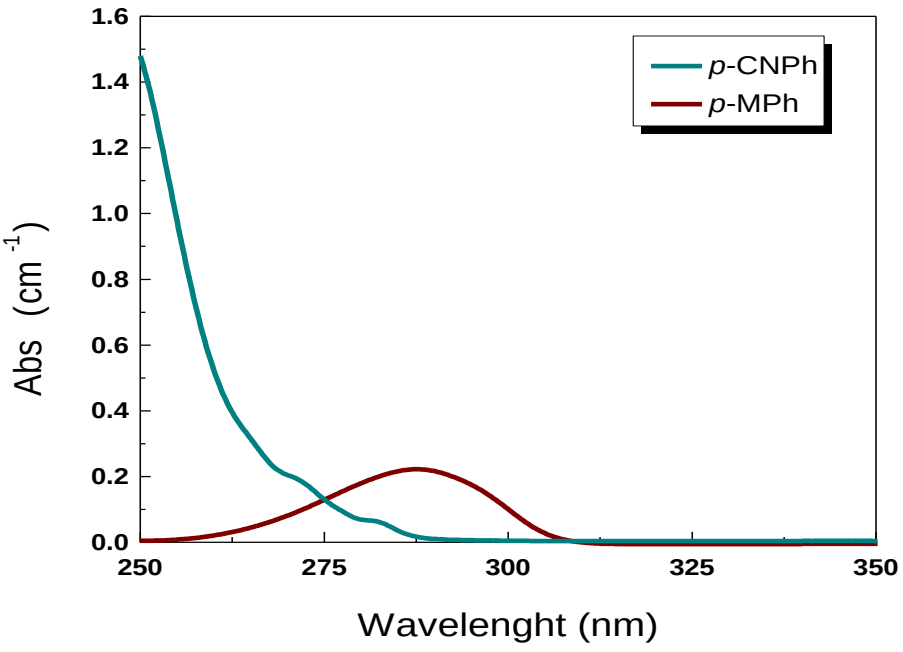

Figure 3.12 - Absorption UV-Vis spectra of 10 mg L^{-1} solutions of *p*-MPh and *p*-CNPh.

3.3.2 Heterogeneous photocatalysis of *p*-Cyanophenol aqueous solutions

The concentration profiles obtained for the degradation of *p*-CNPh using different photocatalysts are represented in Fig. 3.13.

The blank experiment carried out with *p*-CNPh confirms that this probe molecule does not absorb any light from the resulting emission lines of the Heraeus TQ 150 immersion lamp with the optical cut-off of the DURAN 50® filter. The absorption UV-Vis spectrum of a 10 mg L-1 solution of *p*-CNPh (Fig. 3.12) shows that, in fact, no UV-Vis light is absorbed above 295 nm. Therefore, the pollutant degradation is expected to occur under a sensitized photoreaction mechanism.

It was observed that the prepared catalyst which performed better in the degradation of *p*-MPh (0.1SW/CNT) did not show any improvement when compared with bare TiO_2 for *p*-CNPh. Hence, materials prepared under different methods were tested on the photodegradation of *p*-CNPh. In fact, the performance of the catalysts which were subjected to the HT showed an improvement of 40% on the degradation of the model pollutant when compared with the materials prepared by SG without any further treatment.

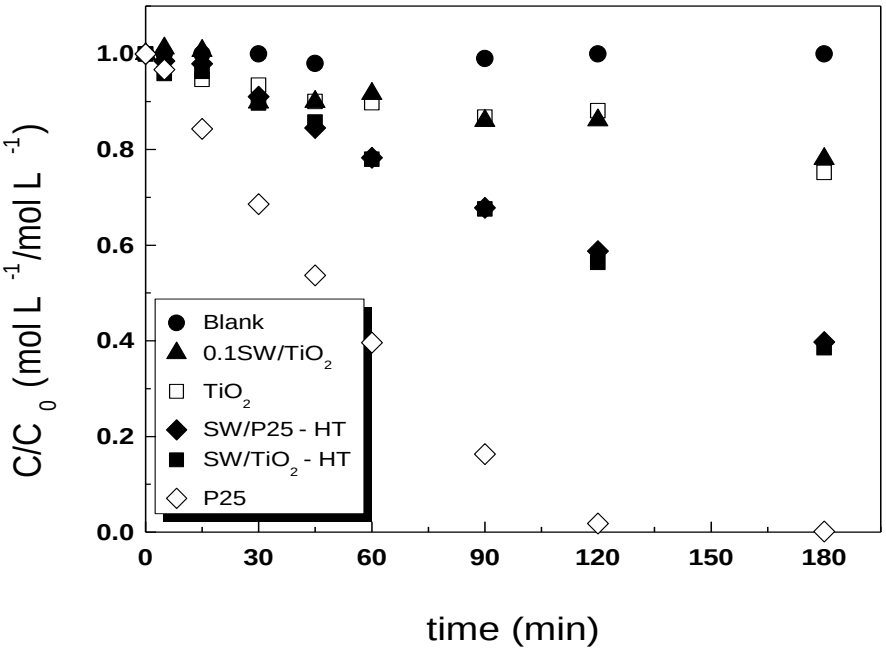

Figure 3.13 - Dimensionless concentration profiles of *p*-CNPh during photocatalytic oxidation reactions using different catalysts.

Regarding the obtained DR UV-Vis spectra for the new materials (SW/TiO_2 – HT and SW/P25 – HT), it can be seen that they absorb light in the visible range (Fig. 3.10). This fact corroborates the better results obtained for these materials, since the experiments are

carried out using a UV-Vis lamp. The higher S_{BET} of the SW/TiO_2 – HT can also contribute to the higher conversions observed. However, the light absorbed by P25 is lower than that of the SW/P25 – HT catalyst in the whole range of the spectrum and the conversion of the pollutant was considerably higher with bare P25 during all the reaction time. In addition, the measured S_{BET} for SW/P25 – HT was higher than for bare P25, and therefore the verified trends can not be only explained with basis on those results. Other issues such as crystalline and amorphous phases should be assessed, for instance using XRD or HRTEM coupled with Selected Area Electron Diffraction (SAED) and Energy-Dispersive X-ray Spectrometer (EDXS) analysis.

In Table 3.6 are gathered the results obtained for TOC and *p*-CNPh conversions. As in the previous case of the *p*-MPh degradation, the pH of the final solution was similar for all the experiments (5.8 ± 0.5) and near the original pH measured for the mother solution (6.3).

Table 3.6 - TOC and *p*-CNPh conversions at the end of irradiation (180 min).

Catalyst	Blank	0.1SW/TiO_2	TiO_2	SW/P25 - HT	SW/TiO_2 – HT
X_{TOC} (%)	0	21	20	47	52
$X_{p\text{-CNPh}}$ (%)	0	22	25	60	62

The obtained pollutant and TOC conversions with TiO_2 and 0.1SW/TiO_2 were lower for *p*-CNPh in comparison with those achieved with *p*-MPh. Since higher photocatalytic efficiencies were observed with the materials subjected to the HT than by SG, the HT methodology should be further explored.

4 Conclusions

The controlled surface modification of SWCNT was successfully performed by means of a HNO_3 hydrothermal functionalization method and the present study allows to draw the following conclusions:

(i) A controlled functionalization using the described HNO_3 hydrothermal method can be achieved by setting with precision the HNO_3 concentration and the temperature.

(ii) The observed dependency in temperature suggests that an activation energy is controlling the functionalization process.

(iii) The functionalization degree on the surface of SWCNT is correlated with the HNO_3 concentration by an exponential function.

(iv) The yield of functionalization over a carbon material and the respective pathway is strongly dependent on their morphologic characteristics.

Preliminary tests on the photocatalytic response of the prepared materials by SG synthesis and some subjected to a HT for the degradation of *p*-MPh and *p*-CNPh, result in the following conclusions:

(v) Previous functionalization of SWCNT on the preparation of SWCNT/TiO_2 composites seems to influence the photocatalytic performance.

(vi) Visible light response in photocatalysis is improved for catalysts which have undergone HT.

(vii) Light absorbance and S_{BET} are insufficient parameters to explain the photocatalytic response of the materials.

5 Future Work

The present work on the development of hybrid SWCNT/TiO_2 photocatalysts is the starting point of a deeper research study that will be held in the context of an European project. Hence, the study is far from being concluded and some future work is suggested for the different issues reported on this thesis.

Functionalization of SWCNT:

It would be interesting to proceed with kinetic studies by performing experiments with different periods of HNO_3 hydrothermal treatment and different temperatures higher than 393 K in order to determine the kinetic parameters of the functionalization process using the HNO_3 hydrothermal approach. In order to avoid high WL during the functionalization treatment, like reported in the current study, pressure and temperature conditions should be optimized. Raman spectroscopy studies are interesting to discuss the optimum time of reaction by evaluating the disorder provoked on the structure of CNT.

Preparation of SWCNT/TiO_2 composites:

The first parameter that must be optimized in the preparation of SWCNT/TiO_2 composites is the amount of SWCNT on TiO_2 matrix by defining the best SWCNT:TiO_2 weight ratio for the photocatalytic oxidative degradation of organic pollutants. Subsequently, the optimum functionalization degree of SWCNT must be found for the previously defined SWCNT:TiO_2 weight ratio. XRD measurements are recommended to assess the dispersion of TiO_2 particles and the crystalline phase composition. Furthermore, different crystalline phase compositions of TiO_2 on SWCNT/TiO_2 composites can be tested by fixing different temperatures of calcination, including the possible interest of amorphous TiO_2. HT over composites prepared by SG approach should be optimized in terms of the solvent used, reaction time, pressure and temperature conditions.

Photocatalytic oxidative degradation of Organic Pollutants:

The first step on further photocatalytic tests is to choose the adequate probe molecule to be studied in terms of no absorption of the emitted radiation by the UV-Vis lamp used. Determination of the optimal catalyst loading, substrate concentration and oxygen partial pressure is of high relevance to establish the conditions over which the screening study of the prepared photocatalysts should proceed.

References

[1] *Directive 2008/105/EC of the European Parliament and of the Council*. 2008, Official Journal of the European Union: Strasbourg.

[2] A. Fujishima, X. Zhang, D.A. Tryk, Heterogeneous photocatalysis: From water photolysis to applications in environmental cleanup. *International Journal of Hydrogen Energy* 32 (2007) 2664-2672.

[3] R. Andreozzi, V. Caprio, A. Insola, R. Marotta, Advanced oxidation processes (AOP) for water purification and recovery. *Catalysis Today* 53 (1999) 51-59.

[4] P.R. Gogate, A.B. Pandit, A review of imperative technologies for wastewater treatment I: oxidation technologies at ambient conditions. *Advances in Environmental Research* 8 (2004) 501-551.

[5] J. Faria, *The Heterogeneous Photocatalytic Process*, in *Catalysis from Theory to Application*, I.d.U.d. Coimbra, Editor. 2008: Coimbra. p. 477-494.

[6] A.L. Linsebigler, G.Q. Lu, J.T. Yates, Photocatalysis on TiO_2 surfaces - principles, mechanisms, and selected results. *Chemical Reviews* 95 (1995) 735-758.

[7] I.A. Montoya, T. Viveros, J.M. Domínguez, L.A. Canales, I. Schifter, On the effects of the sol-gel synthesis parameters on textural and structural characteristics of TiO_2. *Catalysis Letters* 15 (1992) 207-217.

[8] Y.V. Kolen'ko, A.V. Garshev, B.R. Churagulov, S. Boujday, P. Portes, C. Colbeau-Justin, Photocatalytic activity of sol-gel derived titania converted into nanocrystalline powders by supercritical drying. *Journal of Photochemistry and Photobiology A: Chemistry* 172 (2005) 19-26.

[9] O. Carp, C.L. Huisman, A. Reller, Photoinduced reactivity of titanium dioxide. *Progress in Solid State Chemistry* 32 (2004) 33-177.

[10] K. Eufinger, D. Poelman, H. Poelman, R. De Gryse, G.B. Marin, Photocatalytic activity of dc magnetron sputter deposited amorphous TiO_2 thin films. *Applied Surface Science* 254 (2007) 148-152.

[11] Z. Zhang, C.-C. Wang, R. Zakaria, J.Y. Ying, Role of Particle Size in Nanocrystalline TiO_2-Based Photocatalysts. *The Journal of Physical Chemistry B* 102 (1998) 10871-10878.

[12] A. Mills, S. Lee, *Semiconductor photocatalysis*. Parsons S. ed. Advanced Oxidation Processes for Water and Wastewater Treatment. 2004, London: IWA.

[13] W. Wang, P. Serp, P. Kalck, J.L. Faria, Visible light photodegradation of phenol on MWNT-TiO_2 composite catalysts prepared by a modified sol-gel method. *Journal of Molecular Catalysis A: Chemical* 235 (2005) 194-199.

[14] W. Wang, P. Serp, P. Kalck, C.G. Silva, J.L. Faria, Preparation and characterization of nanostructured MWCNT-TiO_2 composite materials for photocatalytic water treatment applications. *Materials Research Bulletin* 43 (2008) 958-967.

[15] Y. Yao, G. Li, S. Ciston, R.M. Lueptow, K.A. Gray, Photoreactive TiO_2/Carbon Nanotube Composites: Synthesis and Reactivity. *Environmental Science & Technology* 42 (2008) 4952-4957.

[16] M.S. Dresselhaus, G. Dresselhaus, A. Jorio, Unusual Properties and Structure of Carbon Nanotubes. *Annual Review of Materials Research* 34 (2004) 247-278.

[17] P. Serp, J.L. Figueiredo, *Carbon Nanotubes and Nanofibers in Catalysis*, in *Carbon Materials for Catalysis*, I. John Wiley & Sons, Editor. 2009, John Wiley & Sons, Inc.: New Jersey. p. 309-372.

[18] M. Ouyang, J.-L. Huang, C.M. Lieber, Fundamental Electronic Properties and Applications of Single-Walled Carbon Nanotubes. *Accounts of Chemical Research* 35 (2002) 1018-1025.

[19] S. Iijima, Helical microtubules of graphitic carbon. *Nature* 354 (1991) 56-58.

[20] S. Iijima, T. Ichihashi, Single-shell carbon nanotubes of 1-nm diameter. *Nature* 363 (1993) 603-605.

[21] D.S. Bethune, C.H. Klang, M.S. de Vries, G. Gorman, R. Savoy, J. Vazquez, R. Beyers, Cobalt-catalysed growth of carbon nanotubes with single-atomic-layer walls. *Nature* 363 (1993) 605-607.

[22] R.H. Baughman, A.A. Zakhidov, W.A. de Heer, Carbon Nanotubes-The Route Toward Applications. *Science* 297 (2002) 787-792.

[23] J.-C. Charlier, Defects in Carbon Nanotubes. *Accounts of Chemical Research* 35 (2002) 1063-1069.

[24] S. Banerjee, T. Hemraj-Benny, S.S. Wong, Covalent Surface Chemistry of Single-Walled Carbon Nanotubes. *Advanced Materials* 17 (2005) 17-29.

[25] K. Balasubramanian, M. Burghard, Chemically Functionalized Carbon Nanotubes. *Small* 1 (2005) 180-192.

[26] J. Garcia, H.T. Gomes, P. Serp, P. Kalck, J.L. Figueiredo, J.L. Faria, Carbon nanotube supported ruthenium catalysts for the treatment of high strength wastewater with aniline using wet air oxidation. *Carbon* 44 (2006) 2384-2391.

[27] C. Baleizão, B. Gigante, H. Garcia, A. Corma, Vanadyl salen complexes covalently anchored to single-wall carbon nanotubes as heterogeneous catalysts for the cyanosilylation of aldehydes. *Journal of Catalysis* 221 (2004) 77-84.

[28] E. Lafuente, M.A. Callejas, R. Sainz, A.M. Benito, W.K. Maser, M.L. Sanjuán, D. Saurel, J.M. de Teresa, M.T. Martínez, The influence of single-walled carbon nanotube functionalization on the electronic properties of their polyaniline composites. *Carbon* 46 (2008) 1909-1917.

[29] V. Datsyuk, M. Kalyva, K. Papagelis, J. Parthenios, D. Tasis, A. Siokou, I. Kallitsis, C. Galiotis, Chemical oxidation of multiwalled carbon nanotubes. *Carbon* 46 (2008) 833-840.

[30] A. Reyhani, S.Z. Mortazavi, A.N. Golikand, A.Z. Moshfegh, S. Mirershadi, The effect of various acids treatment on the purification and electrochemical hydrogen storage of multi-walled carbon nanotubes. *Journal of Power Sources* 183 (2008) 539-543.

[31] M.F.R. Pereira, J.L. Figueiredo, J.J.M. Órfao, P. Serp, P. Kalck, Y. Kihn, Catalytic activity of carbon nanotubes in the oxidative dehydrogenation of ethylbenzene. *Carbon* 42 (2004) 2807-2813.

[32] A. Solhy, B.F. Machado, J. Beausoleil, Y. Kihn, F. Gonçalves, M.F.R. Pereira, J.J.M. Órfão, J.L. Figueiredo, J.L. Faria, P. Serp, MWCNT activation and its influence on the catalytic performance of Pt/MWCNT catalysts for selective hydrogenation. *Carbon* 46 (2008) 1194-1207.

[33] J. Tedim, F. Gonçalves, M.F.R. Pereira, J.L. Figueiredo, C. Moura, C. Freire, A.R. Hillman, Preparation and characterization of poly[Ni(salen)(crown receptor)]/multi-walled carbon nanotube composite films. *Electrochimica Acta* 53 (2008) 6722-6731.

[34] J.S. Noh, J.A. Schwarz, Effect of HNO_3 treatment on the surface acidity of activated carbons. *Carbon* 28 (1990) 675-682.

[35] E. Papirer, J. Dentzer, S. Li, J.B. Donnet, Surface groups on nitric acid oxidized carbon black samples determined by chemical and thermodesorption analyses. *Carbon* 29 (1991) 69-72.

[36] T.J. Bandosz, J. Jagiello, J.A. Schwarz, Comparison of methods to assess surface acidic groups on activated carbons. *Analytical Chemistry* 64 (1992) 891-895.

[37] Y. Otake, R.G. Jenkins, Characterization of oxygen-containing surface complexes crated on a microporous carbon by air and nitric acid treatment. *Carbon* 31 (1993) 109-121.

[38] P.E. Fanning, M.A. Vannice, A DRIFTS study of the formation of surface groups on carbon by oxidation. *Carbon* 31 (1993) 721-730.

[39] P. Vinke, M. van der Eijk, M. Verbree, A.F. Voskamp, H. van Bekkum, Modification of the surfaces of a gas activated carbon and a chemically activated carbon with nitric acid, hypochlorite, and ammonia. *Carbon* 32 (1994) 675-686.

[40] J.A. Menéndez, M.J. Illán-Gómez, C.A.L. y León, L.R. Radovic, On the difference between the isoelectric point and the point of zero charge of carbons. *Carbon* 33 (1995) 1655-1657.

[41] C. Moreno-Castilla, M.A. Ferro-García, J.P. Joly, I. Bautista-Toledo, F. Carrasco-Marín, J. Rivera-Utrilla, Activated carbon surface modifications by nitric acid, hydrogen peroxide, and ammonium peroxydisulfate treatments. *Langmuir* 11 (1995) 4386-4392.

[42] A.C. Apolinário, A.M.T. Silva, B.F. Machado, H.T. Gomes, P.P. Araújo, J.L. Figueiredo, J.L. Faria, Wet air oxidation of nitro-aromatic compounds: Reactivity on single- and multi-component systems and surface chemistry studies with a carbon xerogel. *Applied Catalysis B: Environmental* 84 (2008) 75-86.

[43] H.T. Gomes, B.F. Machado, A. Ribeiro, I. Moreira, M. Rosário, A.M.T. Silva, J.L. Figueiredo, J.L. Faria, Catalytic properties of carbon materials for wet oxidation of aniline. *Journal of Hazardous Materials* 159 (2008) 420-426.

[44] M. Seredych, A.V. Tamashausky, T.J. Bandosz, Surface features of exfoliated graphite/bentonite composites and their importance for ammonia adsorption. *Carbon* 46 (2008) 1241-1252.

[45] L. Calvillo, M.J. Lázaro, E. García-Bordejé, R. Moliner, P.L. Cabot, I. Esparbé, E. Pastor, J.J. Quintana, Platinum supported on functionalized ordered mesoporous carbon as electrocatalyst for direct methanol fuel cells. *Journal of Power Sources* 169 (2007) 59-64.

[46] J.R.C. Salgado, J.J. Quintana, L. Calvillo, M.J. Lázaro, P.L. Cabot, I. Esparbé, E. Pastor, Carbon monoxide and methanol oxidation at platinum catalysts supported on ordered mesoporous carbon: The influence of functionalization of the support. *Physical Chemistry Chemical Physics* 10 (2008) 6796-6806.

[47] P. Serp, M. Corrias, P. Kalck, Carbon nanotubes and nanofibers in catalysis. *Applied Catalysis A: General* 253 (2003) 337-358.

[48] J. Zhang, H. Zou, Q. Qing, Y. Yang, Q. Li, Z. Liu, X. Guo, Z. Du, Effect of Chemical Oxidation on the Structure of Single-Walled Carbon Nanotubes. *The Journal of Physical Chemistry B* 107 (2003) 3712-3718.

[49] A.M.T. Silva, B.F. Machado, J.L. Figueiredo, J.L. Faria, Controlling the surface chemistry of carbon xerogels using HNO_3-hydrothermal oxidation. *Carbon* 47 (2009) 1670-1679.

[50] W. Wang, P. Serp, P. Kalck, J.L. Faria, Photocatalytic degradation of phenol on MWCNT and titania composite catalysts prepared by a modified sol-gel method. *Applied Catalysis B: Environmental* 56 (2005) 305-312.

[51] J.L. Figueiredo, M.F.R. Pereira, M.M.A. Freitas, J.J.M. Órfão, Modification of the surface chemistry of activated carbons. *Carbon* 37 (1999) 1379-1389.

[52] J.L. Figueiredo, M.F.R. Pereira, M.M.A. Freitas, J.J.M. Órfão, Characterization of Active Sites on Carbon Catalysts. *Industrial & Engineering Chemistry Research* 46 (2007) 4110-4115.

[53] T.G. Ros, A.J.v. Dillen, J.W. Geus, D.C. Koningsberger, Surface Oxidation of Carbon Nanofibres. *Chemistry - A European Journal* 8 (2002) 1151-1162.

[54] D.-Q. Yang, J.-F. Rochette, E. Sacher, Functionalization of Multiwalled Carbon Nanotubes by Mild Aqueous Sonication. *The Journal of Physical Chemistry B* 109 (2005) 7788-7794.

[55] H. Yu, Y. Jin, F. Peng, H. Wang, J. Yang, Kinetically controlled side-wall functionalization of carbon nanotubes by nitric acid oxidation. *Journal of Physical Chemistry C* 112 (2008) 6758-6763.

[56] A.I. Kontos, I.M. Arabatzis, D.S. Tsoukleris, A.G. Kontos, M.C. Bernard, D.E. Petrakis, P. Falaras, Efficient photocatalysts by hydrothermal treatment of TiO_2. *Catalysis Today* 101 (2005) 275-281.

[57] J. Yu, H. Yu, B. Cheng, M. Zhou, X. Zhao, Enhanced photocatalytic activity of TiO_2 powder (P25) by hydrothermal treatment. *Journal of Molecular Catalysis A: Chemical* 253 (2006) 112-118.